

**ENCAPSULATION OF THERAPEUTIC PROTEIN WITHIN POLYMERIC
NANOFIBER USING CO-AXIAL ELECTROSPINNING**

MOHAMAD MUHAIMIN BIN ZALANI

BACHELOR OF CHEMICAL ENGINEERING (BIOTECHNOLOGY)

UNIVERSITI MALAYSIA PAHANG

UNIVERSITI MALAYSIA PAHANG

BORANG PENGESAHAN STATUS TESIS♦

JUDUL : ENCAPSULATION OF THERAPEUTIC PROTEIN WITHIN
POLYMERIC NANOFIBER USING CO-AXIAL
ELECTROSPINNING

SESI PENGAJIAN : 2011/2012

Saya MOHAMAD MUHAIMIN BIN ZALANI

(HURUF BESAR)

mengaku membenarkan tesis (PSM/~~Sarjana/Doktor Falsafah~~)* ini disimpan di Perpustakaan Universiti Malaysia Pahang dengan syarat-syarat kegunaan seperti berikut :

1. Tesis adalah hakmilik Universiti Malaysia Pahang
2. Perpustakaan Universiti Malaysia Pahang dibenarkan membuat salinan untuk tujuan pengajian sahaja.
3. Perpustakaan dibenarkan membuat salinan tesis ini sebagai bahan pertukaran antara institusi pengajian tinggi.

4. **Sila tandakan (✓)

SULIT

(Mengandungi maklumat yang berdarjah keselamatan atau kepentingan Malaysia seperti yang termaktub di dalam AKTA RAHSIA RASMI 1972)

TERHAD

(Mengandungi maklumat TERHAD yang telah ditentukan oleh organisasi/badan di mana penyelidikan dijalankan)

TIDAK TERHAD

Disahkan oleh

(TANDATANGAN PENULIS)

(TANDATANGAN PENYELIA)

Alamat Tetap: BT 9, KG BKT BALAI

DR. BALU RANGANATHAN

76100 DURIAN TUNGGAL,

Nama Penyelia

MELAKA

Tarikh : _____

Tarikh: _____

CATATAN :

*

Potong yang tidak berkenaan.

**

Jika tesis ini **SULIT** atau **TERHAD**, sila lampirkan surat daripada pihak berkuasa/organisasi berkenaan dengan menyatakan sekali sebab dan tempoh tesis ini perlu dikelaskan sebagai **SULIT** atau **TERHAD**.

♦

Tesis dimaksudkan sebagai tesis bagi Ijazah Doktor Falsafah dan Sarjana secara penyelidikan, atau disertasi bagi pengajian secara kerja kursus dan penyelidikan, atau Laporan Projek Sarjana Muda (PSM).

**ENCAPSULATION OF THERAPEUTIC PROTEIN WITHIN POLYMERIC
NANOFIBER USING CO-AXIAL ELECTROSPINNING**

MOHAMAD MUHAIMIN BIN ZALANI

**A thesis submitted in fulfillment
of the requirements for the award of the degree of
Bachelor of Chemical Engineering (Biotechnology)**

**Faculty of Chemical & Natural Resources Engineering
Universiti Malaysia Pahang**

JANUARY 2012

SUPERVISOR'S DECLARATION

“I hereby declare that I have read this thesis and in my opinion, this thesis is adequate in terms of scope and quality for the award of the degree of Bachelor of Chemical Engineering (Biotechnology)”

Signature :

Name of Supervisor : Dr. Balu Ranganathan

Position :

Date :

STUDENT'S DECLARATION

I hereby declare that the work in this thesis entitled “encapsulation of therapeutic protein within polymeric nanofiber using co-axial electrospinning” is my own except for quotations and summaries which have been duly acknowledged. The thesis has not been accepted for any degree and is not concurrently submitted for award of other degree.

Signature :

Name : Mohamad Muhaimin Bin Zalani

Date : 20 January 2011

To my parents, Zalani Bin Md. Ali and Embah Binti Saad for understanding my dream and passion, and for letting me chase it.

To my siblings; Zubaidah, Mohd Hafiz, Izzatul Atiyah and Nurhafifah Aina for the brotherly and sisterly consultation and advice. I hope that I managed to inspire you all somehow to dream high and chase your dreams.

And to all my friends, in honour of our friendship and memories.

ACKNOWLEDGEMENTS

First and foremost, I am grateful toward ALLAH the almighty for the blessing given to me and for those I love, without which this project would have not been finished.

I would like to take this opportunity to express my utmost gratitude and heartfelt appreciation to my undergraduate research project supervisor, Dr. Balu Ranganathan for his valuable idea, advice, encouragement and dedicated guidance throughout this undergraduate research project. I would also like to thank Professor Seeram Ramakrishna for the invitation he gave for me to do my internship in NUS Nanoscience & Nanotechnology Initiative. Not to forget Dr. Radhakrishnan Sridhar and Dr. Subramaniam Sundarajan for his guidance and teaching on the electrospinning world and for being there to give consultation and ideas to my research. You have thought me well and I hope I can use all the knowledge I gained from you.

My sincere thanks go to all the people who contributed to the success of this project. Last but not least, my heartiest appreciation also extended to my family for their tireless efforts and on-going support no matter in material and financial. All of you are my driving force and source of my inspiration. I believe that if it was not my family willingness to share my problems, strengthen me and be a constant source of encouragement, it would not have been possible to me to achieve my dream.

I do hope that this report will give the readers some insight as to the maze of activities associated with the encapsulation of therapeutic protein within polymeric nanofiber using co-axial electrospinning from its planning stages until the final analysis and report.

ABSTRACT

A drug delivery system is designed to provide a therapeutic agent in the needed amount, at the right time and to the proper location in the body in a manner that optimizes the efficacy, increases compliance and minimizes side effects. In order to study the encapsulation of therapeutic protein within polymeric nanofiber for controlled release using co-axial electrospinning method, a number of main processing parameters were taken into considerations which are formulation of drug loading, polymer and protein concentration and solution flow rate. Polymeric drug delivery device was developed via electrospinning technique using biodegradable Polymer A. Co-axial electrospinning configuration was used to encapsulate various mixtures of Drug 0066, Drug 0360 and also Polymer B as support into the electrospun nanofibers. Using the configuration, two separate solutions flowed through two different capillaries and electrospun through co-axial nozzle configuration setup. The electrified jet will undergo stretching, leading to formation of long and thin thread. When the liquid jet is continuously elongated, the solvent will evaporate. The grounded collector will attract the charged fiber. The morphology of the electrospun nanofibers were analyzed using Field Emission Scanning Electron Microscopy (FE-SEM) and Transmission Electron Microscopy (TEM). The hydrophilicity of electrospun nanofibers were determined using Surface Contact Angle machine. Fourier Transform Infrared Spectrometry (FT-IR) was used to detect the organic group of the electrospun nanofibers. In vitro release studies were conducted to evaluate sustained release potential of the core-sheath structure composite nanofiber. The results showed that the TEM images clearly proved the core/shell structure of nanofibers for the encapsulation of Drug 0066/Drug 0350 within Polymer A. SEM also showed there was an arch appeared within the nanofiber. The present study would provide a basis for further design and optimization of processing conditions to control the nanostructure of core-sheath composite nanofibers and ultimately achieve desired release kinetics of bioactive proteins (e.g., growth factors) for practical tissue engineering applications.

ABSTRAK

Sistem penghantaran dadah direka untuk menyediakan agen terapeutik dalam jumlah yang diperlukan, pada masa yang tepat dan lokasi yang sepatutnya di dalam badan dengan cara yang mengoptimalkan keberkesanan, meningkatkan pematuhan dan mengurangkan kesan sampingan. Dalam usaha untuk mengkaji pengkapsulan protein terapeutik ke dalam nanofiber berpolimer untuk pelepasan terkawal dengan menggunakan electrospinning sepaksi, beberapa parameter utama pemrosesan telah diambil kira untuk formulasi muatan dadah, kepekatan polimer dan protein dan kadar aliran cecair. Peranti penghantaran dadah berpolimerik telah dibangunkan melalui teknik *electrospinning* menggunakan Polimer A yang mudah terurai. Konfigurasi electrospinning sepaksi digunakan untuk mengurung pelbagai campuran Dadah 0066, Dadah 0350 dan juga Polimer B sebagai sokongan kepada nanofiber. Menggunakan konfigurasi ini, dua cecair yang berasingan mengalir melalui dua kapilari yang berlainan dan melalui konfigurasi muncung berpaksi *electrospinning*. Jet elektrik akan menjalani regangan, membawa kepada pembentukan benang yang panjang dan nipis. Apabila jet cecair memanjang secara berterusan, pelarut akan menguap. Alat pengumpul akan menarik serat yang bercas. Morfologi nanofibers dianalisis menggunakan *Field Emission Scanning Electron Microscopy* (FE-SEM) dan *Transmission Electron Microscopy* (TEM). Hydrophilicity nanofiber telah ditentukan menggunakan mesin *Surface Contact Angle*. *Fourier Transform Infrared* Spektrometri (FT-IR) telah digunakan untuk mengesan kumpulan organik nanofiber. Kajian pembebasan *In vitro* telah dijalankan untuk menilai potensi pembebasan dadah di dalam struktur komposit nanofiber. Hasil kajian menunjukkan bahawa imej-imej TEM jelas membuktikan struktur teras/luar nanofiber bagi pengkapsulan Dadah 0066/Dadah 0350 di dalam Polimer A. SEM juga menunjukkan terdapat timbulan muncul dalam nanofiber. Kajian ini akan menyediakan asas bagi reka bentuk dan mengoptimalkan keadaan pemrosesan bagi mengawal struktur nanofibers komposit teras-luar dan akhirnya mencapai kinetik pelepasan yang diinginkan protein bioaktif (contohnya, faktor pertumbuhan) untuk aplikasi secara praktikal dalam kejuruteraan tisu.

TABLE OF CONTENT

	PAGE
DECLARATION	ii
DEDICATION	iii
ACKNOWLEDGEMENT	v
ABSTRACT	vi
ABSTRAK	vii
TABLE OF CONTENT	viii
LIST OF TABLE	xi
LIST OF FIGURES	xii
LIST OF SYMBOLS/ABBREVIATIONS	xiv
CHAPTER 1 INTRODUCTION	
1.1 Background of study	1
1.2 Problem statement	2
1.3 Research objectives	3
1.4 Scope of study	3
1.5 Rationale and significance	4
CHAPTER 2 LITERATURE REVIEW	
2.1 Processes of electrospinning	5
2.2 General set-ups and processing parameters	7
2.2.1 Needle diameter (nozzle)	8
2.2.2 Distance between tip and collector	9
2.2.3 Polymer concentration	10
2.2.4 Solution flow rate (mono-axial electrospinning)	11
2.2.5 Voltage supply	12
2.2.6 Humidity	14
2.3 Co-axial electrospinning	14
2.3.1 Spinneret/nozzle configuration	16
2.3.2 Core/shell flow rate	17

2.4	<i>In vitro</i> release study	18
2.5	Morphology	23
2.5.1	Fiber diameter	23
2.5.2	Surface contact angle measurement	25
2.5.3	Organic group detection	27

CHAPTER 3 METHODOLOGY

3.1	Introduction	29
3.2	Materials	29
3.3	Core and shell solution preparation	29
3.4	Electrospinning setup	31
3.4.1	Mono-axial electrospinning	31
3.4.2	Co-axial electrospinning setup	32
3.5	Electrospinning process	33
3.6	Characterization of electrospun nanofiber	35
3.6.1	Field-emission scanning electron microscopy (FESEM)	35
3.6.2	Transmission electron microscopy (TEM)	36
3.6.3	Surface contact angle measurement	37
3.6.4	Fourier transform infrared spectrometry (FTIR)	37
3.7	<i>In Vitro</i> Release Study	37

CHAPTER 4 RESULT AND DISCUSSION

4.1	Encapsulation of drugs within polymeric nanofiber	40
4.2	Fiber morphology	43
4.3	Characterization of the encapsulation	48
4.4	Surface contact angle	54
4.5	<i>In vitro</i> proteins release study	55

CHAPTER 5 CONCLUSION AND RECOMMENDATION

5.1	Conclusion	57
5.2	Recommendation	58

REFERENCES	59
APPENDICES	63

LIST OF TABLES

TABLE	TITLE	PAGE
4.1	The concentration of shell and core solution used for electrospinning	41
4.2	Range values of controlled parameters	42

LIST OF FIGURES

2.1	Schematic of the electrospinning process	6
2.2	The relationship between the average fiber diameter and the polymer concentration is given	11
2.3	Effect of varying the applied voltage on the formation of the Taylor cone	13
2.4	Experiment setup used for co-axial electrospinning	16
2.5	TEM images of core/shell (A-C) and pure P(LLA-CL) (D) nanofibers	18
2.6	Release performance differences between PCL-r-fitcBSA/PEG and PCL/fitcBSA/PEG	21
2.7	High-resolution SEM images of fitcBSA contained PCL nanofibers after releasing 176 days for both the PCL-r-fitcBSA/PEG and PCL/fitcBSA/PEG nanofibers.	22
2.8	Contact angle measurement: water droplet (2 μ L) on a PCL film, Teflon film, PCL-only fiber membrane and coaxial PCL/Teflon fiber membrane; dodecane droplet (2 μ L) on fiber membranes of PCL-only and coaxial PCL/Teflon.	26
2.9	FTIR spectra demonstrating presence of proteins in the Group I and Group II nanofibers	28
3.1	Preparation of core and shell solution	30
3.2	Mono-axial electrospinning setup	31
3.3	Co-axial electrospinning setup	32
3.4	High voltage power generator to supply positive direct current to the electrospinning setup	34
3.5	Illustration of fabricating core-shell nanofiber via co-axial nozzle	34
3.6	Humidifier to control the humidity inside the electrospinning chamber	35
3.7	Carbon grid preparation for morphological analysis using TEM	36
3.8	The samples were incubated at 37°C with slow stirring condition	38

3.9	Methodology summary for developing polymeric drug delivery system using co-axial electrospun nanofibers	39
4.1	FE-SEM images of Polymer A without drugs encapsulation under 10k magnification and 20k magnification	43
4.2	FE-SEM images of Polymer A with encapsulation of mixture of Drug 0066, Drug 0350 and Polymer B under 10k magnification and 20k magnification	44
4.3	FE-SEM images of Polymer A with encapsulation of mixture of Drug 0066 and Drug 0350 under 10k magnification and 20k magnification	44
4.4	FE-SEM images of Polymer A with encapsulation of Drug 0350 under 10k magnification and 20k magnification	45
4.5	FE-SEM images of Polymer A with encapsulation of mixture of Drug 0066, Drug 0350 and Polymer B under 50k of magnification	46
4.6	Image of core-shell structured nanofibers composed of Polymer A as shell and the mixture of Drug 0066 and Drug 0350 as core under TEM	49
4.7	FT-IR spectra of electrospun of pure Polymer A	51
4.8	FT-IR spectra of electrospun of Polymer A with the encapsulation of mixture of Drug 0066, Drug 0350 and Polymer B	51
4.9	FT-IR spectra of electrospun of Polymer A with the encapsulation of mixture of Drug 0066 and Drug 0350	52
4.10	FT-IR spectra of electrospun of Polymer A with the encapsulation of Drug 0350	52
4.11	Water contact angles of all scaffolds	54

LIST OF SYMBOLS/ABBREVIATIONS

°C	A scale and unit of measurement for temperature
%	Percent
μL	Microliter
μm	Micrometer
cm	Centimeter
g	Gram
kV	Kilovolts
M	Molar
mL	Milliliter
mL/h	Volumetric flow rate
mm/min	Measurement of flow
h	Hour
mol/L	Molar concentration
MW	Molecular weight
nm	Nanometer
wt %	Mass fraction
w/v %	Mass concentration
FE-SEM	Field Emission Scanning Electron Microscopy
TEM	Transmission Electron Microscopy
FT-IR	Fourier Transform Infrared Spectrometry
DMF	Dimethylformamide
PBS	Phosphate buffer saline
TFE	2, 2, 2-Trifluoroethanol
NUSNNI	National University of Singapore Nanotechnology & Nanoscience Initiative
GMP	Good Manufacturing Practise
FDA	Food and Drug Administration

CHAPTER 1

INTRODUCTION

1.1 Background of Study

Nanotechnology by manipulation of characteristics of materials such as polymers and fabrication of nanostructures is able to provide superior drug delivery systems for better management and treatment of diseases. Benito (2006) states, basically, the concept behind drug delivery is to provide more constant concentrations in the organism, and to bring the compound with pharmaceutical activity directly to the site of need in order to enhance the effectiveness of action.

According to Kim and Pack (2006), a wide variety of new, more potent and specific therapeutics are being created in advances in biotechnology. A drug delivery system is designed to provide a therapeutic agent in the needed amount, at the right time and to the proper location in the body in a manner that optimizes the efficacy, increases compliance and minimizes side effects. Due to common problems in drug delivery such as low solubility, high potency and poor stability, it can impact the efficacy and potential of the drug itself. Thus, there is a corresponding need for safer and more effective methods and devices for drug delivery.

One way to bring the active substance to the site of action is to modify their bio-distribution by entrapping them in particulate drug carriers (Benito, 2006). By encapsulating drugs in designed carriers, labile drugs are protected from degradation inside the hostile conditions. Within the concept of drug delivery the mechanism must be taken

into account to design such carrier systems is sustained or controlled the drug delivery. Controlled-release is aimed at obtaining enhanced effectiveness of the therapeutic treatment by minimizing both under- and over-dosing. A frequently desired feature is to achieve a constant level of drug concentration in the blood circulation or at the site of action of the substance, with a minimum of intakes per day and a maximum coverage. Usually drug delivery systems that dissolve, degrade, or are readily eliminated are preferred.

Biodegradable polymers are of great interest since these materials are processed within the body under biological conditions giving degraded sub-units that are easily eliminated by the normal pathways of excretion (Brannon, 1995). According to Yih *et al.* (2006), polymeric nanoparticles are colloidal solid particles with a size range of 10 to 1000nm and they can be spherical, branched or shell structures. Polymeric vesicles could provide a protective environment for protein molecule to deliver them intact to desired targets.

Among many approaches of fabricating nanofibers, electrospinning, which is also known as electrostatic spinning, is perhaps the most versatile process. This technique allows for the production of polymer fibers with diameters varying from 3 nm to greater than 5 μm (Pham *et al.*, 2006). Moreover, it can easily fabricate nanofiber and microfiber meshes from different types of polymer. Due to their unique features such as high surface-to-volume ratio, morphological design flexibility and extracellular matrices structure-like, nanofibers are used as scaffolds for drug delivery and tissue engineering. Low molecular weight drugs and biomolecules such as proteins and nucleic acids can be encapsulated into the electrospun fibers (Xu *et al.*, 2008).

1.2 Problem Statement

Developing protein and peptide-based drugs present challenges to drug delivery scientists because of their unique nature and difficulty in delivery through conventional routes. The delivery of these therapeutic proteins is limited by their fragile structure and frequent monitoring required. Releasing a protein without denaturation when the polymer is

degraded is what the researcher concern about. When protein is released over time, protein instability problems may occur and result in incomplete release even when the polymer has been degraded. Previous studies shown that the co-axial electrospinning gives an impressive successful method to ensure the bioactivity of these proteins is retained. Coaxial electrospinning was developed for simultaneously electrospinning two different polymer solutions into core/shell nanofibers, or encapsulated bioactive molecular and drugs into polymer nanofibers for controlled release (Chen *et al.*, 2010). Varying the processing parameters will effect to the diameter size and protein release profile of the polymeric drug delivery. By investigating this polymeric drug delivery system, it would able to improve therapeutic efficacy by releasing protein at a controlled rate over a period of time.

1.3 Research Objectives

In this study, there are two objectives aligned to achieve the purpose of encapsulation of therapeutic protein within polymeric nanofiber for controlled release using co-axial electrospinning. The objectives are to develop a polymeric drug delivery system using electrospun nanofibers and to characterize the electrospun nanofibers with various mixtures of drugs encapsulation.

1.4 Scope of Study

The study covers of development of a polymeric drug delivery system using electrospun nanofibers and to characterize the electrospun nanofibers with various mixtures of drugs encapsulation. The scope of study of this experiment is categorized to experimental design and parameters evaluation. The design of this experiment is based on co-axial electrospinning setups and mechanisms. Parameters evaluation of this study have been identified after considering these aspects as main limitations – polymer and protein concentration, solution flow rate, voltage supply and distance between nozzle's tip and collector. The morphology of the electrospun nanofibers were analyzed using Field Emission Scanning Electron Microscopy (FESEM) and Transmission Electron Microscopy (TEM). The hydrophilicity of electrospun nanofibers were determined using Surface

Contact Angle machine. Fourier Transform Infrared Spectrometry (FTIR) was used to detect the organic group of the electrospun nanofibers. In vitro release studies were conducted to evaluate sustained release potential of the core-sheath structure composite nanofiber.

1.5 Rationale and Significance

Therapeutic proteins are one of the most important and rapidly growing segments of the pharmaceutical market, with estimated annual world-wide sales of over \$35 billion in 2005 (Martin, 2006). The potential of these electrospun nanofibers in healthcare application is promising, for example as vector to deliver drugs and therapeutics. Electrospun fiber mat provide the advantage of increased drug release due to the increased surface area. According to Jiang *et al.* (2005), the interconnected, three-dimensional porous structure and enormous surface area of electrospun nanofibers prepared from biodegradable polymers have great potential in tissue engineering, drug delivery and gene therapy. This is due to their biodegradability and fiber-forming properties. The significance of this study is the production of polymer nanofiber membranes encapsulated with therapeutic proteins. It is found that using coaxial nozzle configuration in electrospinning, water-soluble therapeutic proteins can be encapsulated into biodegradable non-woven polymer fibers resulted in subsequent controlled release compared with other methods. Encapsulation of protein using electrospun nanofibers has the advantages of being facile, high loading capacity and efficiency, mild preparation condition and steady release characteristics (Jiang *et al.*, 2005).

CHAPTER 2

LITERATURE REVIEW

2.1 Processes of Electrospinning

According to Lu *et al.* (2008), the process of electrospinning is based on the principle that strong electrical force overcomes weaker surface tension of a polymer solution at certain threshold to eject a liquid jet, could trace its root back to the process of electrospray in which small solid polymer droplets are formed. It is a variation of the electrostatic spraying process where high voltage induces the formation of a liquid jet (Rao, 2009). A typical electrospinning setup consists of three major components which are a high voltage power supplier, a syringe with a metal needle connected to a syringe pump, and a grounded conductive collector (Figure 2.1(A)). A polymer solution is loaded into the syringe and the desired flow rate is controlled by the syringe pump.

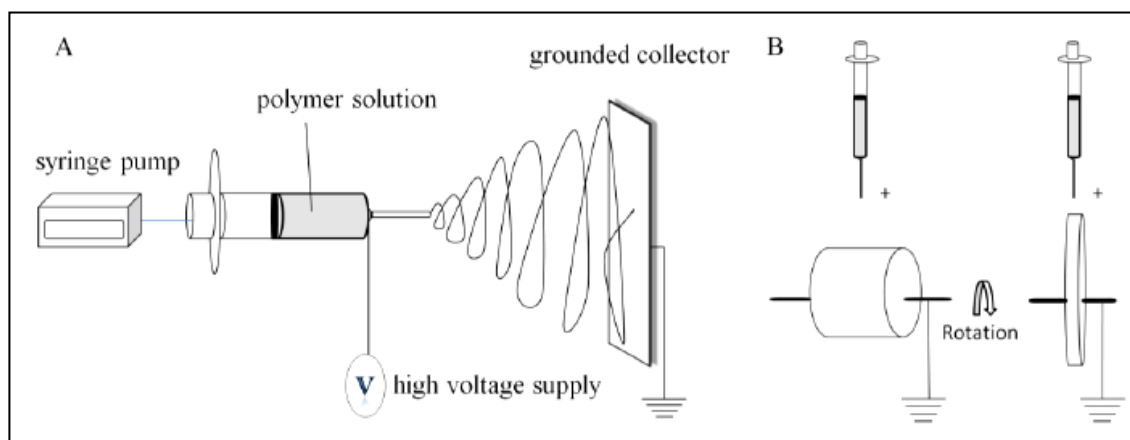


Figure 2.1: Schematic of the electrospinning process. (A) a typical electrospinning set-up and (B) collection methods for creating aligned fibrous scaffolds using rotating drum and rotating disk.

Source: Lee *et al.* 2011

In the electrospinning process, a high voltage is applied to a droplet formed from a polymer solution or melt at the tip of the metal needle. Li *et al.* (2004) explains that the high voltage applied on the nozzle or the needle containing the polymer drop causes it to get highly electrified and the charges are distributed along the surface of the drop evenly. There are two types of electrostatic forces that the drop experiences, namely electrostatic repulsion (b/w surface charges) and the Coulombic force (exerted by external electric field). Doshi and Renekar (1995) explain that these charges undergo mutual repulsion that causes a force which is directly opposite to the surface tension. When the electric field is intensified, elongation of the hemispherical surface of the solution present at the tip of the needle occurs resulting in the formation of a conical shaped structure called as the Taylor cone.

The charging of the fluid leads to the formation of a Taylor cone of the droplet and eventually to the ejection of a liquid jet from the apex of the cone once the strength of electric field has surpassed a certain threshold value. The electrified liquid jet is accelerated

towards the grounded collector by the electric field and thins rapidly due to the evaporation of the solvent and elongation by stretching and whipping. The solidified fiber is often deposited as a randomly oriented, nonwoven mat of nanofibers (Li *et al.*, 2004).

Huang *et al.* (2003) states that further increasing the electric field, a critical value is attained with which the repulsive electrostatic force overcomes the surface tension and the charged jet of the fluid is ejected from the tip of the Taylor cone. The discharged polymer solution jet undergoes an instability and elongation process, which allows the jet to become very long and thin. Meanwhile, the solvent evaporates, leaving behind a charged polymer fiber. In the case of the melt the discharged jet solidifies when it travels in the air.

Based on a review conducted by Pham *et al.* (2006), the shape of the base depends upon the surface tension of the liquid and the force of the electric field; jets can be ejected from surfaces that are essentially flat if the electric field is strong enough. Charging of the jet occurs at the base, with solutions of higher conductivity being more conducive to jet formation. Lee and Arinzeh (2011) justify that the most common method to collect the electrospun nanofibers is on a high speed rotating drum or disk (Figure 2.1(B)). This allows for the fiber to collect along the direction of rotation. Small diameter tubes can also be fabricated by this method and have been used in vascular repair studies. A high rotation speed produces increased fiber alignment as compared to lower rotation speed, but may cause fiber discontinuity.

2.2 General Set-Ups and Processing Parameters

Electrospinning is an efficient, inexpensive technique in which the whole apparatus is compact. The basic set up is a syringe with a metal needle connected to a syringe pump, grounded collector, and a high voltage source. Over the years researchers have found the need to modify the set up for various reasons, but the basic principle has been the same.

Lu *et al.* (2008) states that although the setup for electrospinning is extremely simple, the detailed experimental and theoretical analysis reveals that the electrospinning

process is highly complex. Doshi and Renekar (1995) explain that many parameters can influence the transformation of polymer solution into nanofibers through electrospinning. These parameters include (a) the solution properties such as viscosity, elasticity, conductivity, and surface tension, (b) governing variables such as hydrostatic pressure in the capillary tip, and the gap (distance between the tip and the collecting screen), and (c) ambient parameters such as solution temperature, humidity, and air velocity in the electrospinning chamber.

2.2.1 Needle Diameter (Nozzle)

Rao (2009) elaborates that in electrospinning, a precise amount of polymer solution is taken in the capillary or spinneret. The nozzle (usually the syringe needle set up) determines the amount of polymer melt that comes out, which in turn affects the size of the drop being formed and also the pressure or the amount of force required by the pump so as to push the melt out. If the polymer melt is less viscous, then it can easily come out of the nozzle. The polymer melt is usually a thick highly viscous fluid. So, if the nozzle is too small, then unless it's less viscous, the melt cannot be forced out. Hence, an appropriate nozzle should be chosen. Different types of nozzles or spinnerets have been used over the years. Warner *et al.* (1999) used a spinneret which was basically a stainless steel tube with an outer diameter of 1/16th inch and inner diameter of 0.04 inch. They have also used a capillary of 1.6mm in their experiments.

According to Mo *et al.* (2004), the internal diameter of the needle of the pipette orifice has a certain effect on the electrospinning process. A smaller internal diameter was found to reduce the clogging as well as the amount of beads on the electrospun fibers. The reduction in the clogging could be due to less exposure of the solution to the atmosphere during electrospinning. Decrease in the internal diameter of the orifice was also found to cause a reduction in the diameter of the electrospun fibers. When the size of the droplet at the tip of the orifice is decreased, the surface tension of the droplet increases. Zhao *et al.* (2004) argues that if the diameter of the orifice is too small, it may not be possible to extrude a droplet of solution at the tip of the orifice.

2.2.2 Distance between Tip and Collector

Sill *et al.* (2008) states that the distance between capillary tip and collector can also influence fiber size by 1-2 orders of magnitude. Additionally, this distance can dictate whether the end result is electrospinning or electrospraying. Doshi and Reneker found that the fiber diameter decreased with increasing distances from the Taylor cone. In another study, Jaegar *et al.* (1998) electrospun fibers from a PEO/water solution and examined the fiber diameter as a function of the distance from the Taylor cone. They found that the diameter of the fiber jet decreased approximately 2-fold, from 19 to 9 μm after travelling distances of 1 and 3.5cm, respectively.

The distance between the tip and the collector will have a direct influence in flight time and electric field strength. For fibers to form, the electrospinning jet must be allowed time for most of the solvents to be evaporated. When the distance between the tip and the collector is reduced, the jet will have shorter distance to travel before it reaches the collector plate. The electric field strength will increase at the same time and this will increase the acceleration of the jet to the collector. As a result, there may not have enough time for solvents to evaporate when it reach the collector. When the distance is too low, excess solvents may cause the fibers to merge when they contact to form junctions resulting in intra layer bonding (Ramakrishna *et al.*, 2005).

In a study constructed by Dietzel *et al.* (2001), they had a needle to collector distance of about 20cm while in Warner *et al.* (1999) study, they had a distance of 15cm. Subbiah *et al.* (2004) explains that morphology of the electrospun fibers depends on the evaporation rate, deposition time, and whipping interval. If the distance is too small, it would result in collection of wet fibers and fibers having a bead-like structure. Hence, a suitable distance should be set so that the fibers have enough time to dry.

2.2.3 Polymer Concentration

Sill *et al.* (2008) justifies that polymer concentration determines the spinnability of a solution. The solution must have high enough polymer concentration for chain entanglements to occur. However, the solution cannot be either too dilute or too concentrated. The polymer concentration influences both the viscosity and surface tension of the solution. If the solution is too dilute, the polymer fiber will break up into droplets before reaching the collector due to the effect of surface tension. If the solution is too concentrated, then fibers cannot be formed due to the high viscosity which makes it difficult to control the solution flow rate through the capillary. An optimum range of polymer concentration exists in which fibers can be electrospun when all other parameters are held constant. Figure 2.2 shows that the mean fiber diameter increases monotonically with increasing polymer concentration.

On the other hand, Doshi and Reneker had electrospun fibers from PEO/water solutions containing various PEO concentrations and found that solution with viscosity less than 800 centipoises broke up into droplets upon electrospinning while solutions with viscosity greater than 4000 centipoises were too thick to electrospin. In many experiments it has been shown that within the optimal range of polymer concentrations fiber diameter increases with increasing polymer concentration. Deitzel *et al.* found that fiber diameter of fibers electrospun from PEO/water solution were related to PEO concentration by a power law relationship.

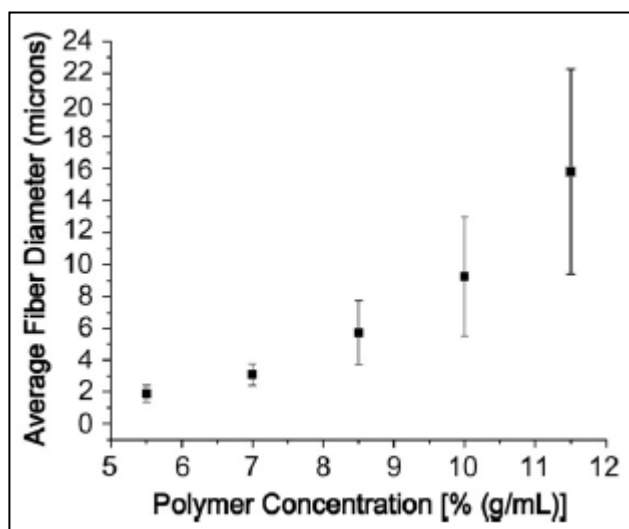


Figure 2.2: The relationship between the average fiber diameter and the polymer concentration is given. Note that the mean fiber diameter increases monotonically with increasing polymer concentration.

Source: Sill *et al.* (2008)

2.2.4 Solution Flow Rate (Mono-Axial Electrospinning)

According to Sill *et al.* (2008), polymer flow rate also has an impact on fiber size, and additionally can influence fiber porosity as well as fiber shape. They state that the cone shape at the tip of the capillary cannot be maintained if the flow of solution through the capillary is insufficient to replace the solution ejected as the fiber jet. Megelski *et al.* examined the effects of flow rate on the structure of electrospun fibers from a polystyrene/tetrahydrofuran (THF) solution. They demonstrated that both fiber diameter and pore size increase with increasing flow rate. Additionally, at high flow rates significant amounts of bead defects were noticeable, due to the inability of fibers to dry completely before reaching the collector. Incomplete fiber drying also leads to the formation of ribbonlike (or flattened) fibers as compared to fibers with a circular cross section.

According to Ramakrishna *et al.* (2005), the flow rate will determine the amount of solution available for electrospinning. For a given voltage, there is a corresponding feed rate if a stable Taylor cone is to be maintained. When the feed rate is increased, there is a corresponding increase in the fiber diameter or beads size. This is due to greater volume of solution that is ejected from the needle tip. Yuan *et al.* (2004) argues that a lower feed rate is more desirable as the solvent will have more time for evaporation. The jet will take a long time to dry due to the greater volume of solution drawn from the needle tip.

The rate at which the polymer comes out of the needle/nozzle is an important factor in electrospinning. Doshi and Reneker (1993) filled a capillary tube with the polymer solution and a hydrostatic pressure was established by an air pump which was controlled by valves and was read on a manometer. Warner *et al.* (1999) used a digitally controlled, positive displacement syringe pump (Harvard Apparatus PHD 2000) and had typical flow rates ranging between 0.2 ml/min to 1 ml/min. Dietzel *et al.* (2001), used a flow rate of 0.05ml/hr achieved using a Harvard 2000 syringe pump. Subbiah *et al.* (2004) mentioned that the material transfer rate and the jet velocity are directly dependent on this feature. They have also mentioned that researchers have found that the higher the polymer flow rate, bigger the diameter of the fibers.

2.2.5 Voltage Supply

One of the most studied parameters among the controlled variables is the effect of field strength or applied voltage. Rao (2009) explains that a suitable high voltage is applied on the needle such that, when it exceeds a critical value, the drop which is induced at the tip of the needle distorts into the shape of a cone and a charged jet of the polymer erupts from the apex of this cone. This jet gets drawn towards the grounded collector by the electric field. Similarly, Warner *et al.* (1999) used a Gamma High Voltage Research ES30-P power supply to induce a voltage up to 20 kV in their experiments. Dietzel *et al.* (2001) found this critical value to be 5 kV. They have applied voltages ranging from 5kV-15kV in their experiments.

According to Pham *et al.* (2006), at low voltages or field strengths, a drop is typically suspended at the needle tip, and a jet will originate from the Taylor cone producing bead-free spinning (assuming that the force of the electric field is sufficient to overcome the surface tension). As the voltage is increased, the volume of the drop at the tip decreases, causing the Taylor cone to recede. The jet originates from the liquid surface within the tip, and more beading is seen. As the voltage is increased further, the jet eventually moves around the edge of the tip, with no visible Taylor cone. At these conditions, the presence of many beads can be observed.

Similarly, Sill *et al.* (2008) explains that at relatively low applied voltages, a pendant drop (depicted in light gray) is formed at the tip of the capillary as shown in Figure 2.3. The Taylor cone (depicted in dark gray) then forms at the tip of the pendant drop. However, as the applied voltage is increased (moving from left to right), the volume of the pendant drop decreases until the Taylor cone is formed at the tip of the capillary. Increasing the applied voltage further results in the fiber jet being ejected from within the capillary that is associated with an increase in bead defects.

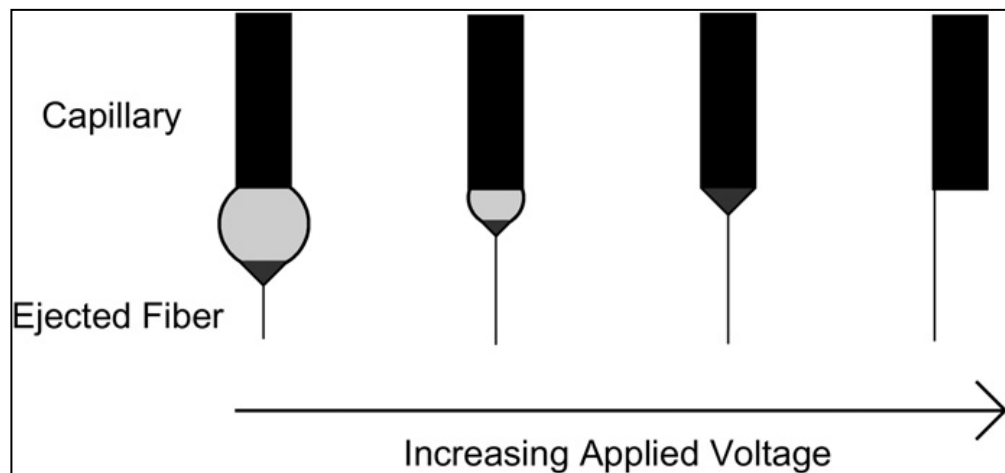


Figure 2.3: Effect of varying the applied voltage on the formation of the Taylor cone.

Source: Sill *et al.* 2008

2.2.6 Humidity

The humidity was varied by Casper *et al.* (2004), while spinning polystyrene solutions. Their work showed that increasing the humidity resulted in the appearance of small circular pores on the surface of the fibers and further increasing the humidity will lead to the pores coalescing as determined by atomic force microscopy. At high humidity, it is likely that water condenses on the fiber surface when electrospinning is carried out under normal atmosphere. As a result, this may have an influence on the fiber morphology especially polymers dissolved in volatile solvents (Megelski *et al.*, 2002). According to him, water vapor may condense on the jet surface due to jet surface cooling as a result of rapid evaporation of the volatile solvent. Pores are created when both water and solvent eventually evaporate. Pores seen on electrospun fibers mat due to the dynamic condition of the electrospinning jet as compared to static condition

The humidity of the environment will also determine the rate of solvent evaporation of the solvent in the solution. At a very low humidity, a volatile solvent may dries very rapidly. The solvent evaporation may be faster than the removal of the solvent from the needle tip. As a result, the electrospinning process may only be carried out for a few minutes before the needle tip is clogged (Ramakrishna *et al.*, 2006).

2.3 Co-Axial Electrospinning

In many cases, the application of nanofibers is required to keep the functionalizing agents (for example, biomolecules such as enzymes, proteins, drugs, viruses, and bacteria) in the fluid environment to maintain their functionality. In order to meet this requirement, core-shell nanofibers were prepared by a modified electrospinning process, co-axial electrospinning. According to Yarin (2010) in his review, he mentions that co-axial electrospinning or co-electrospinning of core-shell micro- and nanofibers was born 7 years ago as a branch of nanotechnology which bifurcated from a previously known electrospinning. Through electrospinning, co-electrospinning inherited roots in polymer science and electrohydrodynamics, while some additional genes from textile science and

optical fiber technology were spliced in addition. He also states that co-electrospinning rapidly became widely popular and its applications proliferated into such fields as biotechnology, drug delivery and nanofluidics. It also triggered significant theoretical and experimental efforts directed at a better understanding and control of the process.

According to Chakraborty *et al.* (2009), the emergence of coaxial electrospinning has allowed the development of many new designs of functional nanotechnological materials. Co-axial electrospinning is a simple and rapid technique to produce micro or nanotubes, drug or protein loaded nanofibers and hybrid core-shell nanofibrous materials. The greatest advantage of coaxial electrospinning is its versatility in the type (hydrophobic or hydrophilic) and size (ranging from 100 nm to 300 μm) of fibers it can produce. Mono-axial electrospun fibers have been reported to be able to incorporate and release antibiotics, drugs and proteins in a sustained manner. However, the distribution and release of drugs from the fibers are poorly controlled. Moreover, growth factors and cytokines embedded in polymer matrixes also suffer from significant decrease in bioactivity. Coaxial electrospun fibers as delivery system for tissue engineering offer better drug stability, more complete drug encapsulation and tighter control of release kinetics as compared to mono-axial fibers.

Wang *et al.* (2009) explains that co-axial electrospinning is not limited to the production of core-shell nanofibers with a continuous core. Core-shell droplet can also be generated by coaxial electrospinning. A co-axial jet of hydrophilic polymer (outside) and a hydrophobic liquid (inner) is electrospun, produces beaded fibers, encapsulating the hydrophobic liquid into these beads. In this case, the beads are regularly distributed along the fibers, and their sizes exhibit a uniform distribution. Both the bead to bead distance and fiber diameter may be controlled by the outer liquid flow rate, while the bead diameter can be adjusted by controlling the inner liquid flow rate.

2.3.1 Spinneret/Nozzle Configuration

Guorui and Wei (2011) mention that the setup of co-axial electrospinning adopted by most researchers is quite similar to that used for basic electrospinning, but a modification is made in the spinneret.

Figure 2.4 shows the difference modified spinneret of coaxial electrospinning setup by difference researches in their reports. In co-electrospinning reviewed by Yarin (2010), a plastic syringe with two compartments containing different polymer solutions or a polymer solution (shell) and a non-polymeric Newtonian liquid or even a powder (core) is used to initiate a core-shell jet (Figure 2.4(A)). At the exit of the core-shell needle attached to the syringe appears a core-shell droplet, which acquires a shape similar to the Taylor cone due to the pulling action of the electric Maxwell stresses acting on liquid. Liquid in the cone, being subjected to sufficiently strong (supercritical) electric field, issues a compound jet, which undergoes the electrically driven bending instability characteristic of the ordinary electrospinning process. Strong jet stretching resulting from the bending instability is accompanied by enormous jet thinning and fast solvent evaporation. As a result, the core-shell jet solidifies and core-shell fibers are depositing on a counter-electrode.

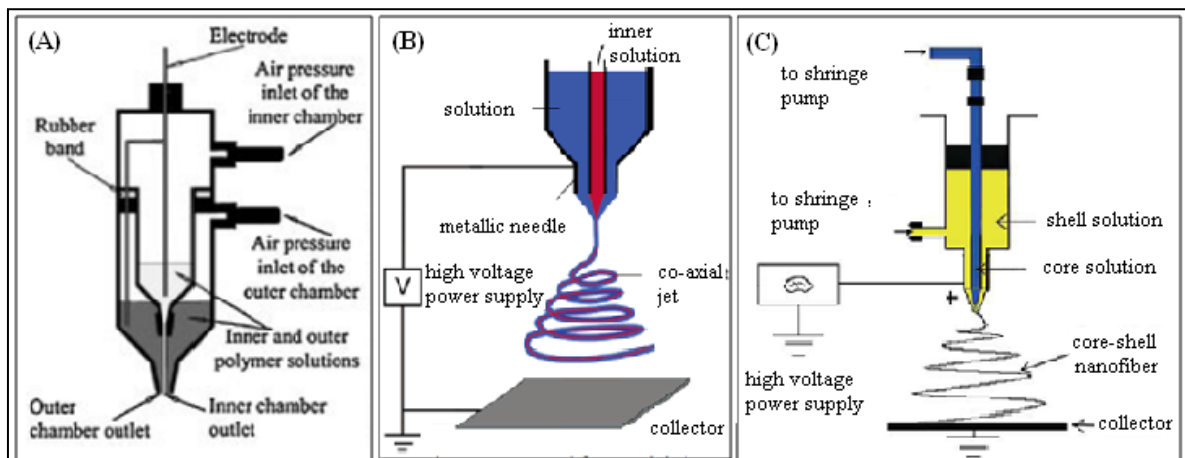


Figure 2.4: Experiment setup used for co-axial electrospinning (A) by Yarin (2010), (B) Gourui and Wei (2011) and (C) Sahoo *et al.* (2009).

Figure 2.4(B) shows the modified spinneret by Gourui and Wei (2011) study, in which a smaller (inner) capillary is inserted concentrically in to a bigger (outer) capillary to create a coaxial configuration. This coaxial configuration allows for the simultaneous electrospinning of two different polymer solutions, with the outer needle attached to the syringe containing the shell solution and the inner connected to the syringe holding the core solution. When the polymer solutions are charged using a high voltage, the charge accumulation occurs predominantly on the surface of the sheath liquid coming out of the outer coaxial capillary. The pendant droplet of the sheath solution elongates and stretches due to the charge-charge repulsion to form a conical shape, and once the charge accumulation reaches a certain threshold value due to the increased applied potential, a fine jet extends from the cone. The stresses generated in the sheath solution cause shearing of the core solution via ‘viscous dragging’ and ‘contact friction’. This causes the core liquid to deform into a conical shape and a compound coaxial jet develops at the tip of the cones.

According to Sahoo *et al.* (2009) in their study of encapsulation of bFGF within PLVA polymer, they used a modification of the electrospinning technique using two concentric needles (Figure 2.5(C)) to spin two immiscible solutions into coaxial fibers which proteins have been incorporated into the core of such nanofibers. Such a method protects the protein from the organic solvent used to dissolve the outer polymer coat, and also enables electrospinning of a protein solution that is otherwise not “electrospinnable”.

2.3.2 Core/Shell Flow Rate (Co-Axial Electrospinning)

The morphology and the size of the core/shell of the electrospun nanofiber are really affected to the flow rate of the core and shell solution. According to the study conducted by Chen *et al.* (2010), when the proportion of feeding rate in process of fabrication between inner solution and outer solution were 1:3, TEM investigations clearly proved the core/shell nanofiber of nanofibers. As shown in the Figure 2.5, the TEM image (Figure 2.5(A)) clearly proved the core/shell structure of P(LLA-CL)-Heparin compared with pure P(LLA-CL) nanofiber (Figure 2.5(D)). Besides that, the diameter of core layer

increases with increasing feeding rate of inner solution. However, the overloading of inner solution could lead the presence of beads (Figure 2.5(C)).

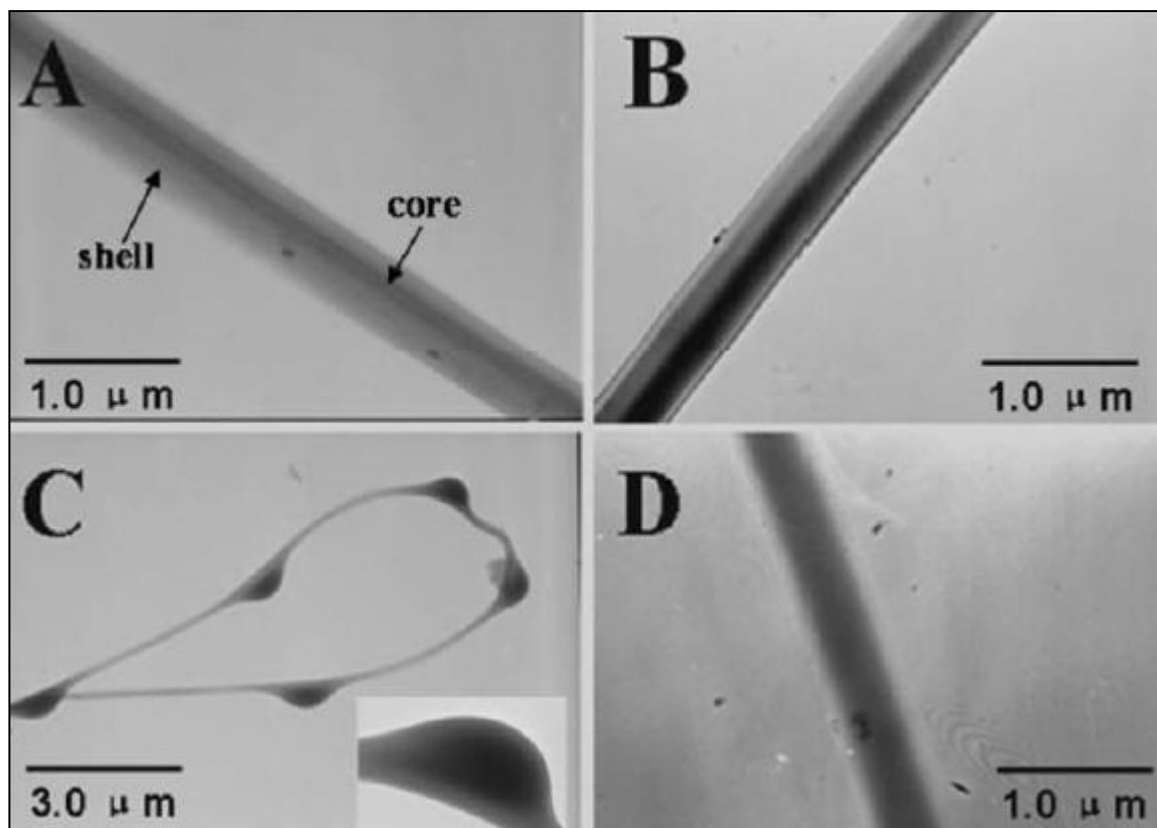


Figure 2.5: TEM images of core/shell (A-C) and pure P(LLA-CL) (D) nanofibers. The proportions of feeding ratios between inner solution and outer solution were (A) 1:3, (B) 1:2 and (C) 1:1.

Source: Chen *et al.* 2010

2.4 *In Vitro* Release Study

Zhang *et al.* (2006) explains that many important factors (e.g., the protein properties, coencapsulated molecules, polymer matrix, and the interactions among them, etc.) have influences on the drug/protein release kinetics. Encapsulation by formation of

core-sheath compounded nanofibers will provide an alternative strategy for moderating the release rate of drug release. Notably, it would be more effective than other forms of devices due to its nanoscale size, which implies less possibility of introducing fabrication-related defects and higher surface area for mass transfer, and protective function for preserving the activity of the agents encapsulated.

In their study, the release performance differences between PCL-r-fitcBSA/PEG and PCL/fitcBSA/PEG were plotted in Figure 2.6 and compared on the basis of the same protein loadings. The release kinetics for all cases can be illustrated by two stages: an initial fast release before the inflections (stage I) followed by a constant linear release (stage II). In stage I, there were initial burst releases from both composite nanofibers with averaged release amounts of 35.7% in 3 h for PCL/fitcBSA/PEG and 31.2% in 4 h for PCL-r-fitcBSA/PEG. Burst release in PCL/fitcBSA/PEG is obviously more severe than that of encapsulation formulation. After this initial burst release, protein was approximately linearly released (stage II) with PCL-r-fitcBSA/PEG being released faster than that of PCL/fitcBSA/PEG. If it is assumed that the intercepts of the linear curves were associated with the burst release phenomena, it was found that the initial fast release in a period of 2 days for the composite nanofibers of PCL/fitcBSA/PEG blend accounts for 60-70%, versus 45-65% for the core-sheath-structured PCL-r-fitcBSA/PEG. Incorporation of BSA by blending-electrospinning is worse than that for the encapsulation mode. Encapsulation therefore would suppress the burst release.

The suppression efficiency versus flow rate (loadings) was plotted in Figure 2.6(D). The perfect linearity indicates the suppression efficacy is proportional to the loadings. This is understandable as smaller loading in terms of current blending formulation is almost equivalent to an encapsulation effect, while higher loading will be able to form channels for agent to release faster from the device. After the initial fast release, both formulations were able to release proteins at constant releasing rates. However, sustainability between both formulations is different. PCL/fitcBSA/PEG could not sustain a sufficient amount of release over a long time, resulting in reduced effective lifetime of the releasing device. For example, before their common intersection points of the linear ranges are reached,

encapsulated release devices, that is, the core-shell-structured nanofibers, can sustain a higher amount of releases of 27-35%. In contrast, the incorporated ones support only about 10-20%.

At the end of the *in vitro* release study (approaching 100%), both the PCL-r-fitcBSA/PEG and PCL/fitcBSA/PEG nanofibers were observed by high-resolution SEM. Interestingly, the fiber morphology of PCL/fitcBSA/PEG (Figure 2.7d-f) has changed from previously smooth surfaces (images not shown) to very rough and eroded-like with very obvious pits and/or cavities presented. The severity is obviously related to the incorporated amount of fitcBSA/PEG. Since the fitcBSA/PEG aggregates are water-soluble, it is believed that the pits/cavities were formed from the dissolution of the fitcBSA/PEG aggregates presented on and in the fiber. However, this did not happen for the coaxial electrospun PCL-r-fitcBSA/PEG nanofibers. The only change, compared to its pristine form, is that the PCL-r-fitcBSA/PEG fibers became flatter and collapsed from their previous cylindrical shape (Figure 2.7a-c). This may arise from the exhausted state of fitcBSA/PEG aggregates inside the PCL shell. The different post-release morphologies in both composite nanofibers would therefore relate to their respective distribution manners of the fitcBSA/PEG aggregates in the composite nanofibers due to different techniques used for nanofiber preparations, and consequently different delivery fashions or mechanisms during the *in vitro* releasing process.

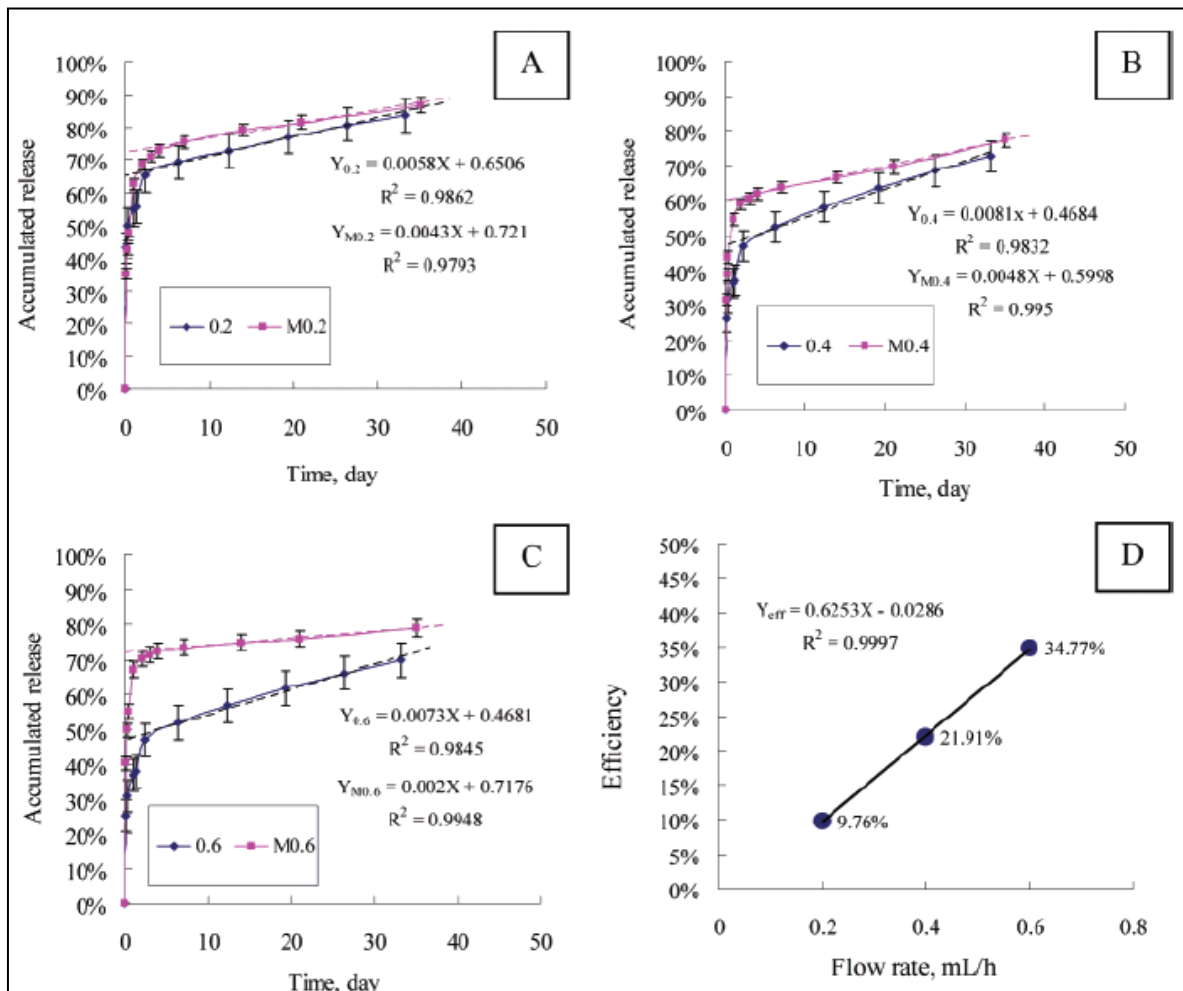


Figure 2.6: Release performance differences between PCL-r-fitcBSA/PEG and PCL/fitcBSA/PEG

Source: Zhang *et al.* 2006

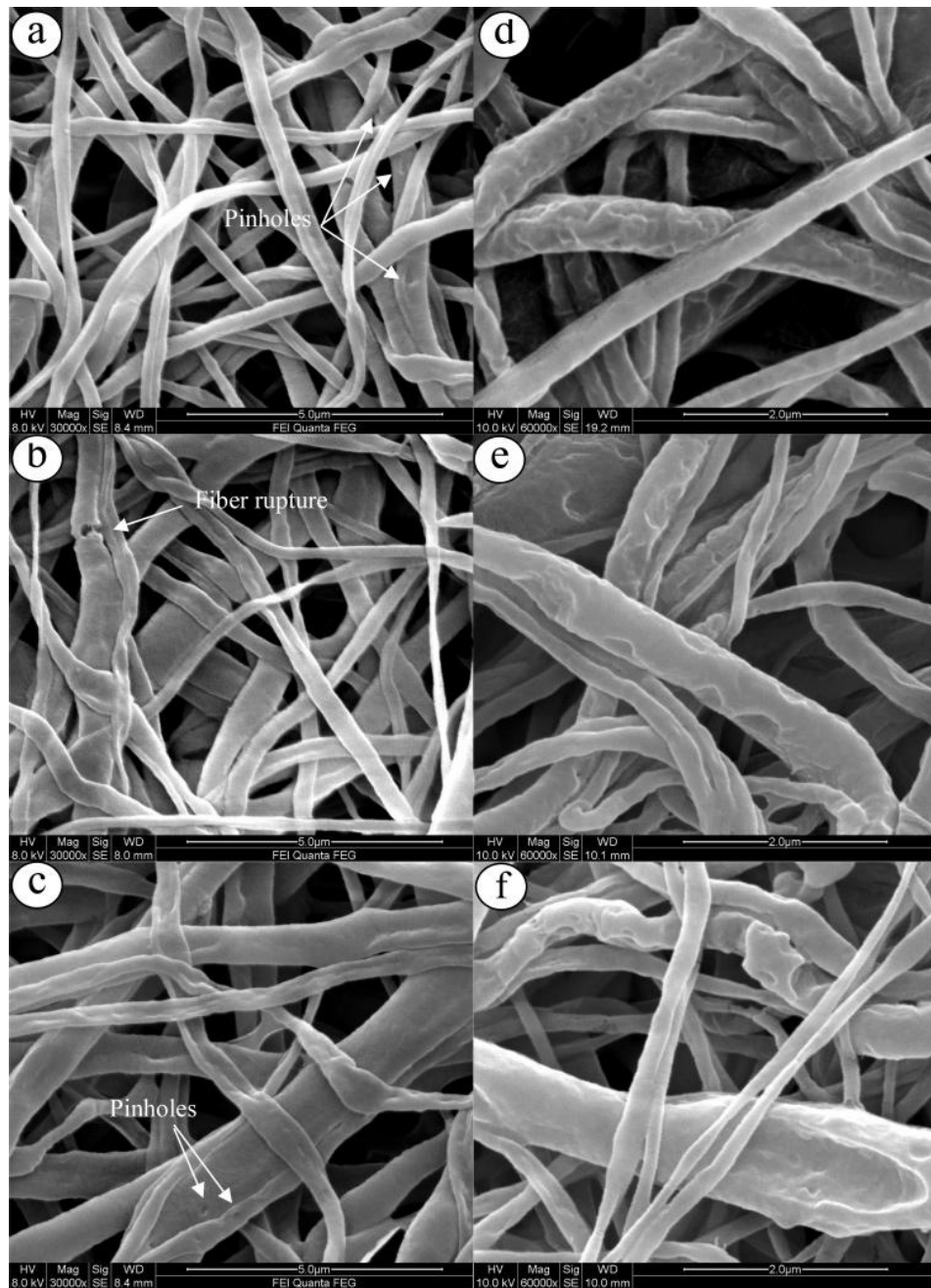


Figure 2.7: High-resolution SEM images of fitcBSA contained PCL nanofibers after releasing 176 days for both the PCL-r-fitcBSA/PEG and PCL/fitcBSA/PEG nanofibers.

Source: Zhang *et al.* 2006

2.5 Morphology

According to Ramakrishna *et al.* (2006), the morphology of the electrospun nanofibers can be characterized by scanning electron microscope (SEM), field emission SEM (FE-SEM) and transmission electron microscope (TEM). Since nanofiber membranes have porous structure, morphological properties include pore geometry and density.

2.5.1 Fiber Diameter

Scanning electron microscopy (SEM) creates magnified images by using electron beams to observe the electrospun nanofiber diameter. Rao (2004) justifies that, in SEM, as the samples are illuminated with electrons, they have to be made to be conductive so that they can bounce off the electrons. A sample of electrospun nanofiber can easily be made conductive by coating it with a thin layer of gold in a gold sputtering machine. The samples are then placed into the SEM chamber and the air is pumped out of the chamber creating a vacuum. An electron gun positioned at the top of the set-up emits a beam of high energy electrons which travels down the column through a series of magnetic lenses designed to focus the beam to a very fine spot. The beam hits the sample producing secondary electrons and these backscattered electrons are collected by a secondary detector, converted to a voltage, and amplified. This amplified voltage is displayed on a cathode ray tube (CRT) and this display corresponds to the surface topography as well as morphology of the sample. The advantage of using SEM over conventional light microscopy is that SEM offers high resolution of images, thus even very closely spaced features can be studied.

While conventional SEM requires a high vacuum in the specimen chamber to prevent atmospheric interference with the electrons, field emission SEM (FE-SEM) can be operated even with poor vacuum (as much as 10 Torr of vapor pressure) in the specimen chamber. For this “environmental” aspect to be incorporated, the upper and lower portions of the vacuum column should be totally isolated from the specimen chamber. The imaging gas in this equipment is water vapor (Rao, 2004). In this regard, FE-SEM is highly recommended to observe electrospun nanofibers (Casper *et al.*, 2004). According to Rao

(2004), the main advantage of FE-SEM over SEM is the fact that the material need not be made conductive by coating with gold or palladium and so the sample's original characteristics may be preserved for further testing. The sample can also be modified and imaged later as its original characteristics have not been altered by a conductive coating. Also, as the field-emission gun produces a brighter primary electron beam, its accelerating voltage may be lowered significantly, thus permitting imaging of even fragile samples.

Ramakrishna *et al.* (2006) explains that in the electrospinning process, polymer solution is stretched by electrical charge difference between the needle tip and the ground collector. While polymer jet is travelling to the collector, solvent is evaporated. After electrospinning, residual solvent may still exist on the nanofibers. Electrospun nanofibers are dried at least one night under vacuum condition. From a completely dried nanofiber membrane, an area of 1 cm x 1 cm is cut and attached by means of carbon tape to a copper stub. It is important at this juncture to ensure that direct adhesion of nanofibers is not recommended since adhesive of carbon tape may damage the nanofibers. This is especially so if the biodegradable polymer nanofibers are treated.

Another important concern in observing ultrafine nanofibers is the thickness of the conductive gold coating. The thickness of gold coating generally is around 25 nm. If the ultrafine nanofibers are examined under SEM, coating thickness interrupts the accuracy of diameter measurement. To avoid the coating influence, the nanofiber diameter is measured under transmission electron microscopy (TEM). In a TEM, the electron source is generally tungsten filament heated with a low voltage source. The filament is held at a large negative potential and the electrons are accelerated towards specimen with less than 100 nm thick. Similar to SEM, X-ray escapes from material surface and the detected X-ray supplies the information of particular element of the sample. After the electron beam passes through the sample, transmitted beams accordingly passes through the other lenses and finally an image is produced. A metal mesh is subjected to coating and fine supporting polymer film is placed on the metal mesh. The carbon coating is then further applied to the metal mesh and nanofibers are electrospun on the mesh. Gold coating is not necessary for a TEM

sample. TEM observation is a useful methodology to accurately measure the diameter of ultrafine nanofibers (Ramakrishna *et al.*, 2006).

2.5.2 Surface Contact Angle Measurement

Surface contact angle of electrospun nanofibrous membranes is simply examined by a water contact angle (WCA) machine. A distilled water pendent droplet is injected from a syringe onto the membrane surface. The image of the droplet on the membrane is visualized through the image analyzer and the angle between the water droplet and the surface is measured. Hydrophilic materials show low contact angle (spreading of water across surface) while hydrophobic materials show high contact angle (minimal contact between droplet and surface) (Ramakrishna *et al.*, 2006).

Conversely, to reduce the hydrophobicity and make a surface more hydrophilic, surface modification techniques have to be employed. Fujihara *et al.* (2005) tried to applied hydrophobic polycaprolactone (PCL) nano fibrous scaffolds as bone grafting material. However, the problem was hydrophobic scaffolds were not suitable for osteoblast attachment and proliferation. Hence, air plasma treatment was adopted to enhance the hydrophobicity of PCL nano fibrous scaffolds. The plasma treatment for 10 minutes decreased the surface contact angle of membranes to zero value. This was possible because plasma treatment introduced polar chemical groups onto the scaffold surface, increasing the surface energy of polymer and thereby decreasing in surface contact angle.

In a study conducted by Han and Steckl (2009), they have measured the contact angle to superhydrophobic and oleophobic fibers. Contact angle examples on different substrates are shown in Figure 6. The left-hand panels in Figure 2.8 are typical of liquid-solid interactions on the relatively smooth surface of thin films. The water droplet on spin-coated PCL and a Teflon AF film exhibits contact angles of 69° (hydrophilic) and 120° (hydrophobic), respectively. On coaxially electrospun fiber membranes, the water droplet is either in the Cassie-Baxter state or the metastable Cassie-Baxter state, and the contact angle is increased as a result of surface roughness and entrapped air within the fibers. As shown

in the center panels of Figure 2.8, the PCL fiber membrane results in a CA of 125° , and the coaxial PCL/Teflon fiber membrane produces a CA of 158° (superhydrophobic). Interestingly in their study, the coaxially electrospun fiber membrane shows oleophobicity whereas the PCL-only fiber membrane is oleophilic. As shown in the right-hand panels of Figure 2.8, when a $2\ \mu\text{L}$ droplet of dodecane ($\sim 23\ \text{mN/m}$) is placed on the electrospun PCL-only fiber membrane, the dodecane spreads thoroughly and its contact angle is almost 0° . However, on the coaxially electrospun PCL fiber coated with Teflon AF the dodecane droplet has a contact angle of $\sim 130^\circ$, preventing oil spreading.

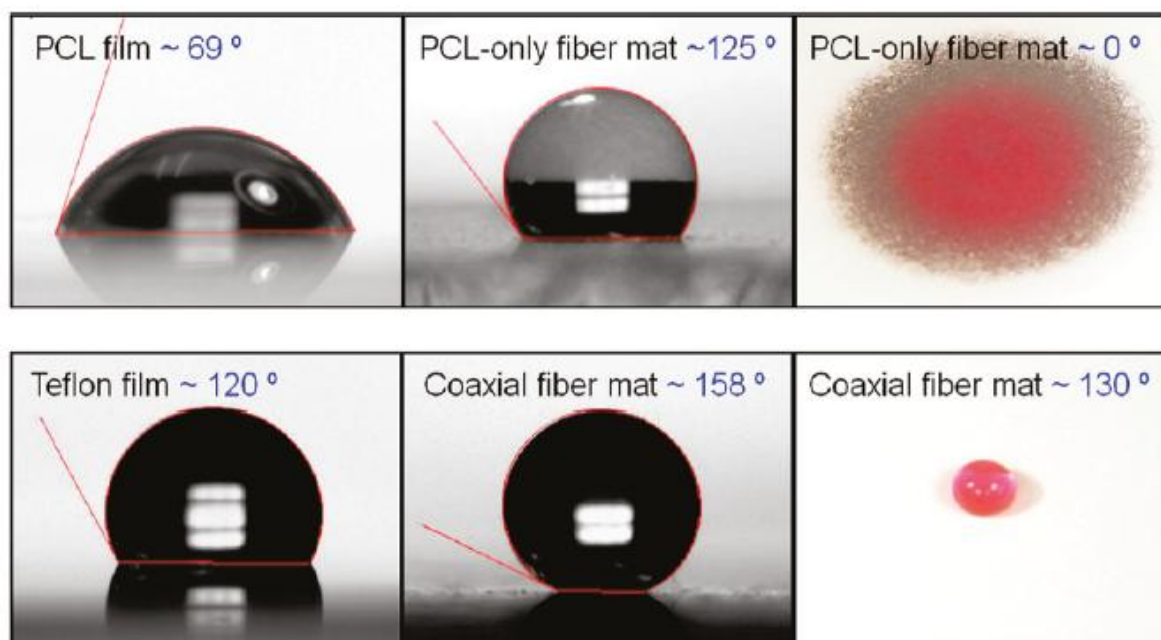


Figure 2.8: Contact angle measurement: water droplet ($2\ \mu\text{L}$) on a PCL film, Teflon film, PCL-only fiber membrane and coaxial PCL/Teflon fiber membrane; dodecane droplet ($2\ \mu\text{L}$) on fiber membranes of PCL-only and coaxial PCL/Teflon.

Source: Han and Steckl 2009

2.5.3 Organic Group Detection

Cambell *et al.* (2000) justifies that for functional group detection on electrospun nanofibers, Fourier-Transform Infrared Spectroscopy (FTIR) is utilized. As infrared frequency corresponds to molecular frequency, infrared spectroscopy sensitively reflects molecular structure of material. Two cases (influence by spinning process and chemical or physical reaction after spinning) are found to investigate chemical functional groups which exist in electrospun nanofibers. As to the influence by the spinning process, the concern is how the chemical structure of polymer is influenced by electrospinning process. After making electrospun nanofibers, certain applications may require surface modification to attach chemical function on the nanofiber surface (Ramakrishna *et al.*, 2006).

Sahoo *et al.* (2009) examined their two modifications of the electrospinning technique to develop bFGF-releasing PLGA nanofibers, fabricated by blending and electrospinning (Group I) or by coaxial electrospinning (Group II) using FTIR. The studies indicated that protein was incorporated in both groups of nanofibers; the presence of additional peaks at 1635 and 1644 cm^{-1} , corresponding to protein Amide I and at 1534 cm^{-1} , corresponding to protein Amide II is characteristic of proteins (Fig. 4). The peaks were more prominent on the Group I fibers, presumably due to a more superficial arrangement of the proteins on these fibers. All nanofibers had a characteristic peak at 1758 cm^{-1} corresponding to C=O stretch in the PLGA molecule.

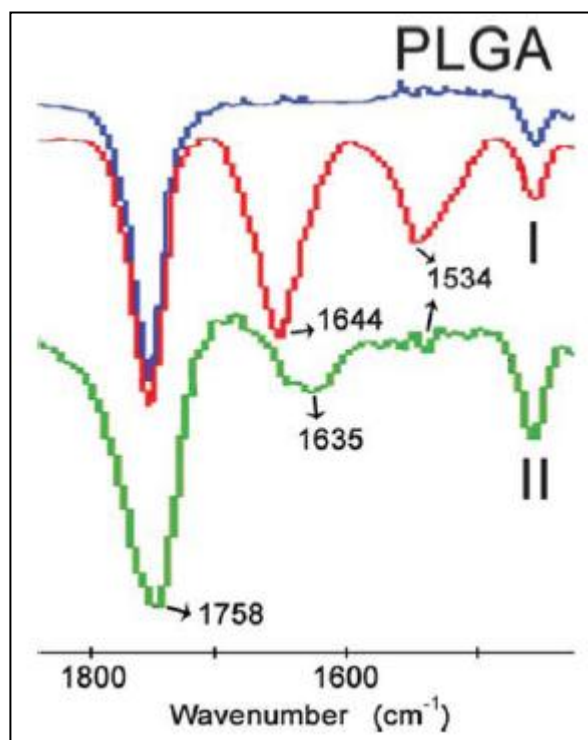


Figure 2.9: FTIR spectra demonstrating presence of proteins in the Group I (in red) and Group II nanofibers (in green) indicated by characteristic protein Amide-I peaks (1635/1644 cm⁻¹) and protein Amide II peaks (1534 cm⁻¹) that are absent in the spectral plot of pure PLGA nanofibers (in blue).

Source: Sahoo *et al.* 2009

CHAPTER 3

METHODOLOGY

3.1 Introduction

This chapter will discuss the experimental design used to encapsulate the therapeutic protein within polymeric nanofiber, the characterization of the electrospun nanofibers incorporated with multiple proteins and the multiple proteins release profiles from the protein-loaded electrospun nanofibers.

3.2 Materials

Polymer A and Polymer B were purchased from Aldrich (St. Louis, USA). Drug 0350 and Drug 0066 were procured from Sigma-Aldrich (St. Louis, USA). All the chemicals used are of analytical grade and used without further purification.

3.3 Core and Shell Solution Preparation

0.500g of Drug 0066 was dissolved in 10ml of distilled water and 30.2mg of Drug 0350 was dissolved in 10ml of ethanol solvent. 5wt% of Polymer B was prepared by dissolving 1.5015g of Polymer B in 28.5ml of distilled water and the solution was stirred at 60°C overnight. The core solutions were obtained by the various mixtures of Drug 0066, Drug 0350 and Polymer B as support and were stirred for several hours for homogenous purpose.

The shell solution was obtained by dissolving Polymer A in two different ways of solvents used. The first shell solution was prepared by dissolving 1.007g of Polymer A in 5ml of chloroform and 3ml of methanol to produce 10wt% of Polymer A solution. The second one was prepared by dissolving 1.212g of Polymer A in 10ml of 2, 2, 2-Trifluoroethanol (TFE) to produce 12w/v% of Polymer A. The polymer solutions were stirred for an overnight to ensure that the solutions have sufficient viscosity for electrospinning (Figure 3.1).

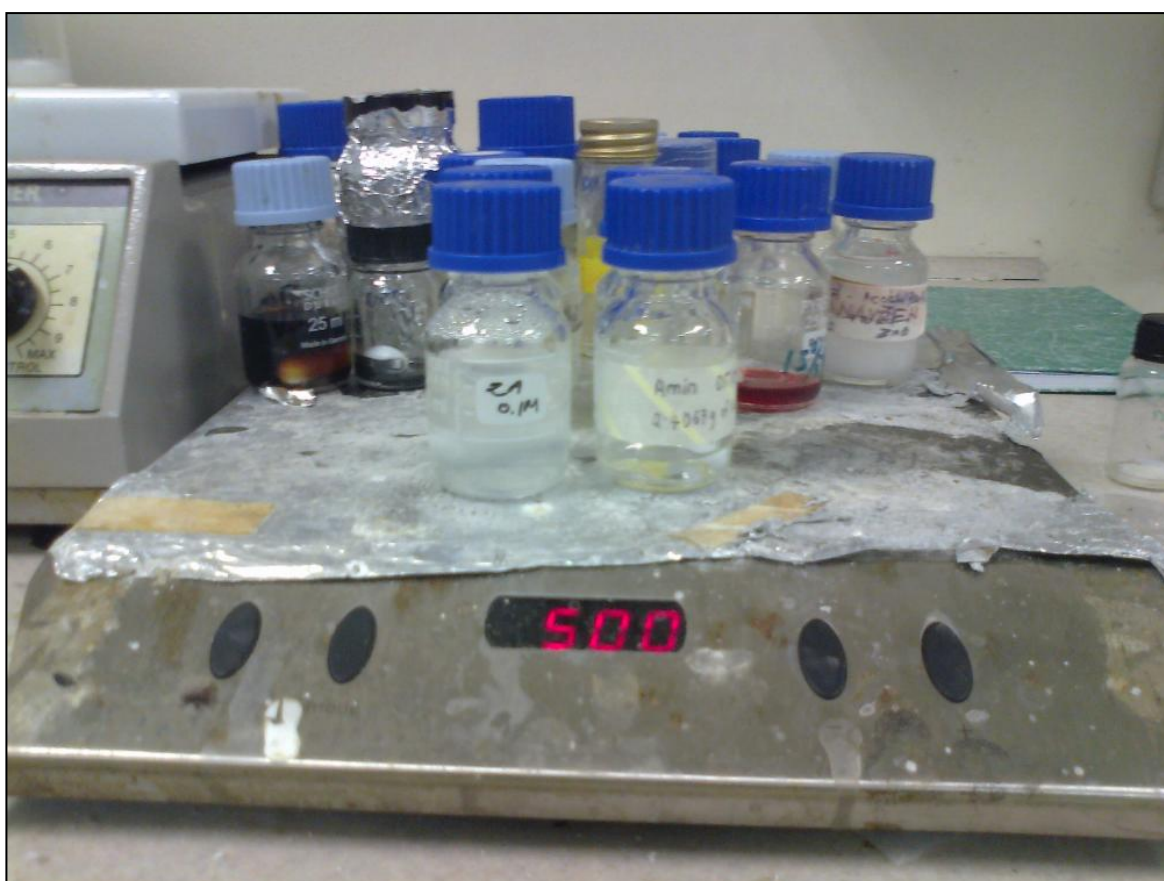


Figure 3.1: Preparation of core and shell solution

3.4 Electrospinning Setup

Both mono-axial and co-axial electrospinning setup were used for this study. Mono-axial electrospinning was used to fabricate Polymer A as control for this experiment while co-axial electrospinning was used as main study procedure to fabricate the co-axial nanofiber.

3.4.1 Mono-Axial Electrospinning

The mono-axial electrospinning setup used in this experiment was obtained from Dr. Radhakrishnan Sridhar of NUSNNI. As shown in Figure 3.2, 18G needle (Becton Dickinson & Company, USA) was attached to a syringe (Becton Dickinson & Company, USA). The syringe was located to the syringe pump (Kd Scientific, Singapore) to control the polymer solution flow rate.



Figure 3.2: Mono-axial electrospinning setup

3.4.2 Co-Axial Electrospinning Setup

The co-axial electrospinning setup used in this experiment was obtained from Dr. Radhakrishnan Sridhar of NUSNNI. For this setup, the co-axial nozzle configuration of 25G needle for inner and 16G needle for outer capillary's size was used. The needles of 25G and 16G were attached together in the co-axial nozzle. Each of the two co-axial electrospinning setup channels is connected to two syringes (Becton Dickinson & Company, USA) using Teflon tubes and the two syringes are connected to two syringe pumps (Kd Scientific, Singapore) to control the core and shell solutions flow rate.



Figure 3.3: Co-axial electrospinning setup. Co-axial nozzle configuration was used with 2 different sizes of needles were attached to it and the flow rates of the solutions were controlled by the syringe pumps.

3.5 Electrospinning Process

In a typical co-axial electrospinning, Polymer A solution was added to the syringe connected to the metallic needle, and the drug component was added to another syringe connected to the inner capillary of the co-axial nozzle. These two liquids were fed at a constant rate through syringe pumps. The feed rate for the Polymer A solution was varied from 1.4 ml/h to 1.8 ml/h while the drug compound's feed rate was varied from 0.1 ml/h to 0.6 ml/h. The metallic needle was connected to a high-voltage power supply. High voltage regulated direct current power supply was used as in Figure 3.4. The collector, a piece of aluminum foil covered on an electrical grounded metal plate, was placed about 13 cm to 14 cm below the tip of the metallic needle. The Polymer A penetrated within the drug solution that was connected to another syringe forming the core-shell solution (Figure 3.5). All connections were sealed with cellophane tape. The typical voltage range for electrospinning was 10–19 kV. The electrospinning was conducted under ambient conditions with humidity in the range of 54% to 70% controlled by humidifier as shown in Figure 3.6. While the electrospinning process was operating, some of the electrospun nanofiber was collected to observe the morphology under light microscope. Parameters were controlled until fine nanofibers contain no beads and spindles were formed. The collected scaffolds were stored in vacuum overnight at room temperature to eliminate solvent residuals.



Figure 3.4: High voltage power generator to supply positive direct current to the electrospinning setup

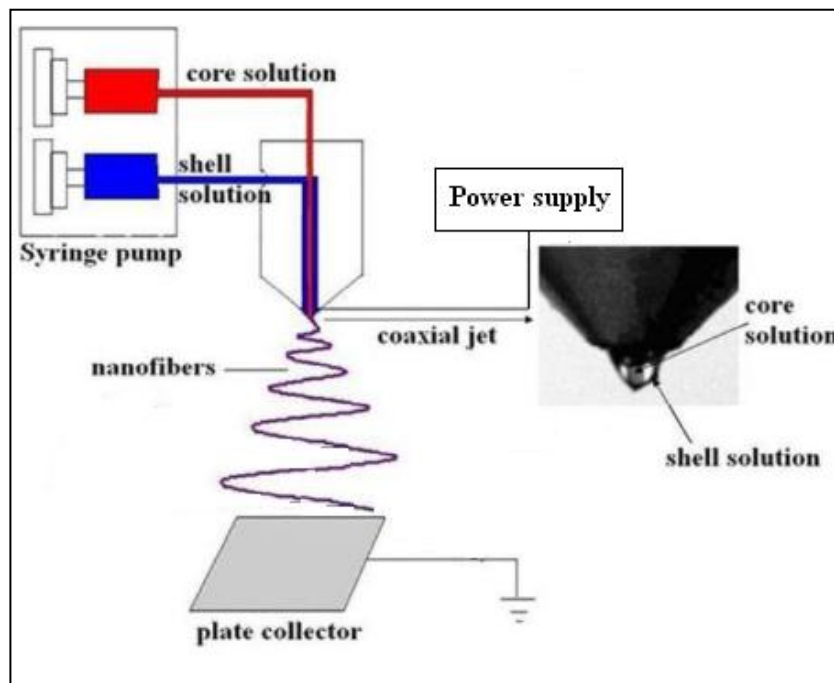


Figure 3.5: Illustration of fabricating core-shell nanofiber via co-axial nozzle.



Figure 3.6: Humidifier to control the humidity inside the electrospinning chamber

3.6 Characterization of Electrospun Nanofiber

The electrospun nanofibers were characterized using Field-emission Scanning Electron Microscopy (FE-SEM), Transmission Electron Microscopy (TEM), Surface Contact Angle machine and Fourier Transform Infrared Spectrometry (FTIR).

3.6.1 Field-emission Scanning Electron Microscopy (FE-SEM)

The electrospun nanofibrous membranes, mounted on metal stubs by using conductive double-sided tape, were sputter-coated with platinum up to 60s in a fine coater. Their morphologies were then observed through Field-emission SEM (JEOL JSM-6701F

FESEM) which equipped with cold field emission electron source with magnification from 25 to 650 000 times and accelerating voltage from 0.5kV to 30kV.

3.6.2 Transmission Electron Microscopy (TEM)

The core-shell structure of the fibers was observed by Transmission Electron Microscopy (JEOL JEM 3010 TEM). The samples for TEM were prepared by directly depositing the as-spun nanofibers onto copper grids as shown in Figure 3.7. The samples were kept in a vacuum oven for 48 hours for drying at room temperature before TEM imaging.



Figure 3.7: Carbon grid preparation for morphological analysis using TEM

3.6.3 Surface Contact Angle Measurement

Surface contact angle was determined by water drop measurement of Visual Contact Angle (VCA) Optima by using electrospun nanofiber mats as the substrates.

3.6.4 Fourier Transform Infrared Spectrometry (FT-IR)

To determine the quality or consistency of the samples, Fourier Transform Infrared Spectrometry (FT-IR) is used. After the background sample has been measured, the sample was put into the spectrometer and measured. The measured signal was digitized and sent to the computer as final infrared spectrum to be interpreted.

3.7 *In Vitro* Release Study

The electrospun nanofiber mats samples were first measured using analytical measurement. The samples were then cut, so that each of their weight was about 35-37mg. The samples were transferred into the vials. 15ml of phosphate buffer saline (PBS) solution (0.05 M, pH 7.4) was added into each vial. All vials contained samples were incubated with slowly stirred at 37°C inside the incubator as shown in Figure 3.8. At predetermined time interval, 1ml of the release medium was collected and analyzed.



Figure 3.8: The samples were incubated at 37°C with slow stirring condition.

In summary the methodology to develop a polymeric drug delivery system using Polymer A electrospun nanofibers for controlled release of various mixtures of drugs can be summarized as below.

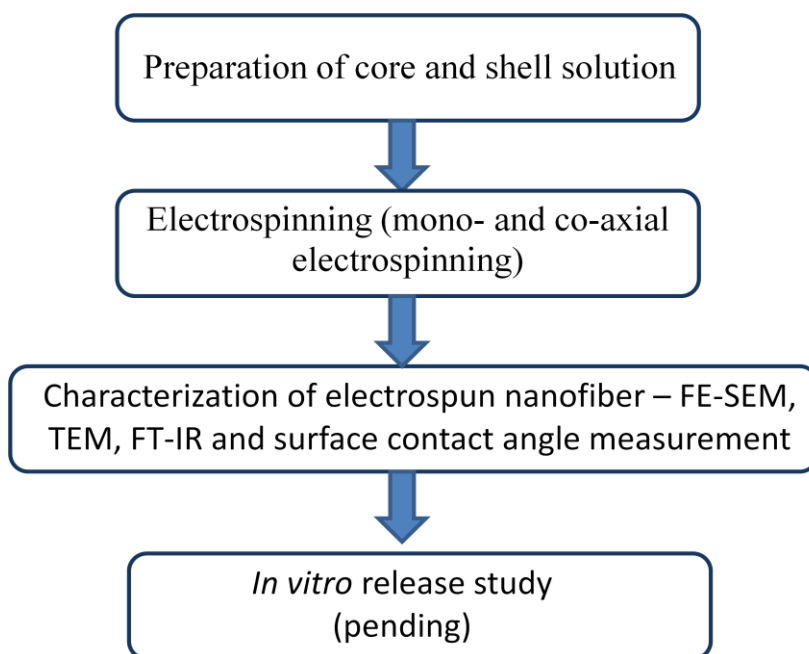


Figure 3.9: Methodology summary for developing polymeric drug delivery system using co-axial electrospun nanofibers.

CHAPTER 4

RESULTS AND DISCUSSION

4.1 Encapsulation of Drugs within Polymeric Nanofiber

In terms of forming a fibrous structure, the pure Drug 0066 and Drug 0350 were found to be nonelectrospinnable. This is due the fragility property of these bioagent products that need to be preserved to maintain their bioactivity from the electrospinning process. However, this would not be a prerequisite for generating nanofibers in the co-axial electrospinning process, as the major role in fiber forming would be the shell solution used. Polymer A was used as model polymer to shell structure of the electrospun nanofibers while Polymer B was used as support to stabilize the composition of various mixtures of drugs inside the shell.

Based on several papers that have been reviewed, concisely, Polymer A was obtained by dissolving in two different ways of solvents used. The first shell solution was prepared by dissolving 1.007g of Polymer A in 5ml of chloroform and 3ml of methanol to produce 10 wt % of Polymer A solution. The second one was prepared by dissolving 1.212g of Polymer A in 10ml of 2, 2, 2-Trifluoroethanol (TFE) to produce 12 w/v % of Polymer A. These different ways were used to determine which one of them can produce more stable and regular fibrous structure. The results showed that, 12 w/v % of Polymer A by dissolving in 10ml of TFE yields a better fibrous compared to dissolving in chloroform and methanol.

In order to produce well aligned structure of electrospun nanofibers from co-axial electrospinning process, the concentration of each material was investigated. The alignments were observed under 50 times magnification of light microscope. The concentrations of Polymer A and various concentrations of mixture of Drug 0066, Drug 0350, and Polymer B that were used to produce fine nanofiber using co-axial electrospinning setup is shown in the Table 4.1. The result showed that for the shell solution, 12 w/v % of Polymer A is the best concentration that can be used to form well aligned structure of electrospun nanofibers to encapsulate variety composition of core solutions. However, there are different concentrations of various composition of core solution used to form well aligned structure of electrospun nanofibers. As control procedure for this study, mono-axial electrospinning was also been used to electrospin the Polymer A.

Table 4.1: The concentration of shell and core solution used for electrospinning

Shell Solution (Polymer A Concentration, w/v %)	Core Solution	
	Composition	Concentration
12	Drug 0066/Drug 0350/Polymer B	5 wt %
12	Drug 0066/Polymer B	10 wt %
12	Drug 0066/Drug 0350	5 wt %
12	Drug 0350	0.4 w/v %

As core and shell solutions were able to be electrospun through co-axial electrospinning configuration, the concentrations used were manage to entangle the solution chains and overcome the solution surface tension. The formation of stable Taylor cone during electrospinning process indicates that the voltage supply used was acceptable as the electrostatic force in the solution was generated to overcome the solution surface tension. The feed rate used for both core and shell solutions were sufficient to produce fine fibers even though small diameter beads were seen in the electrospun fibers. The distance used in the electrospinning process to produce the electrospun nanofibers were able to

allow enough time for the solvents to evaporate when it reach the collector. As pore diameters on the electrospun fibers were not clearly seen, it can be said that the humidity used in the electrospinning process was acceptable.

The well aligned structure of electrospun nanofibers are determined by various processing parameters including shell/core concentration, voltage supply, shell/core solutions flow rate, distance between the needle tip to collector and needle diameter. Electrical potential and core/shell concentration are the key factors governing the fiber diameter, apparent density and porosity. Overall morphology, degradation rate and matrix characteristics of the electrospun nanofiber can be tailored by controlling electrospinning parameters and polymer blend composition. Table 4.2 shows the range value of parameters that need to be controlled and maintained throughout the electrospinning process to produce well aligned structure of electrospun nanofibers.

Table 4.2: Range values of controlled parameters

Parameter	Range Values
Shell concentration	1.4 ml/h to 1.8 ml/h
Core concentration	0.1 ml/h to 0.6 ml/h
Voltage supply	10 kV to 19 kV
Distance between nozzle's tip and collector	13 cm – 14 cm
Humidity	54 % to 70 %

Encapsulation of various mixtures of Drug 0066, Drug 0350 and also Polymer B as support into biodegradable Polymer A was successfully electrospun using co-axial electrospinning technique. Compared to the mono-axial electrospinning technique, coaxial electrospun fibers are able to distribute and release proteins in a sustained manner. The core-shell design allows bioagents Drug 0066, Drug 0350 and also Polymer B as support to dissolve in aqueous solution for encapsulation. Using reservoir-type structure, the core-

shell structure ensures that the drug enclosed in the polymer matrix and the proteins is concentrated in the core of the fibers as opposed to the random distribution of the proteins in the fiber matrix. This will guarantee in better control over the release kinetics of the proteins.

4.2 Fiber Morphology

Shown in Figure 4.1 is the nanofibrous morphologies of electrospun Polymer A without drugs encapsulation using mono-axial electrospinning under 10k and 20k magnification of FE-SEM. This polymer was electrospun to be as control for this study. The process was run under controlled parameters with 12 wt % of concentration, 15kV of power supply, 1.2ml/h of flow rate and 14 cm of the distance between nozzle's tip and collector. All fibers demonstrated a large diameter with the average around 1 μ m with no beads formed. However, the morphology of the electrospun nanofibers showed the fibers were not deposited in uniform at the ground collector. It is suspected that the applied voltage of 15kV is not sufficient to form uniformly fibers. Depending on the feed rate of the solution, a higher voltage may be required so that the Taylor Cone is stable thus yield uniformly fibers.

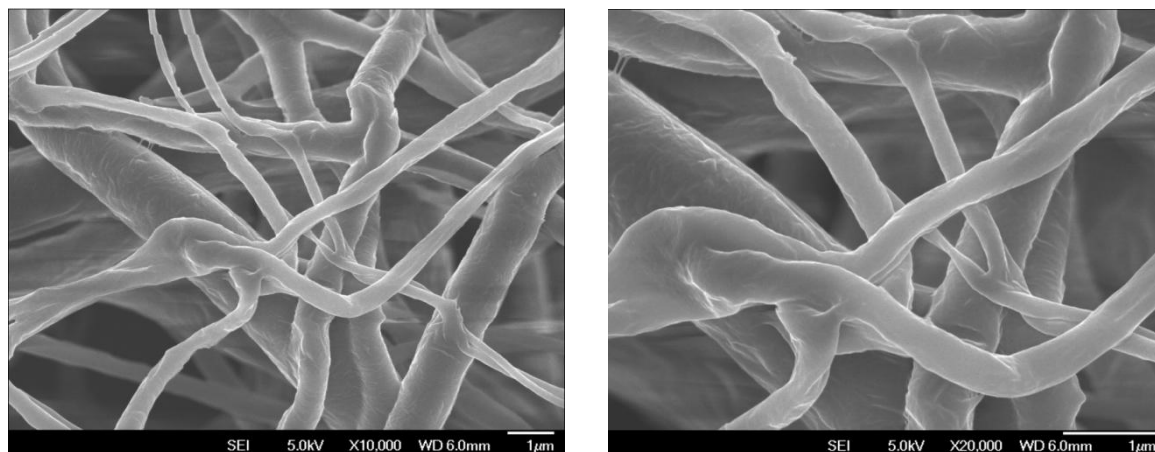


Figure 4.1: FE-SEM images of Polymer A without drugs encapsulation under 10k magnification (left) and 20k magnification (right).

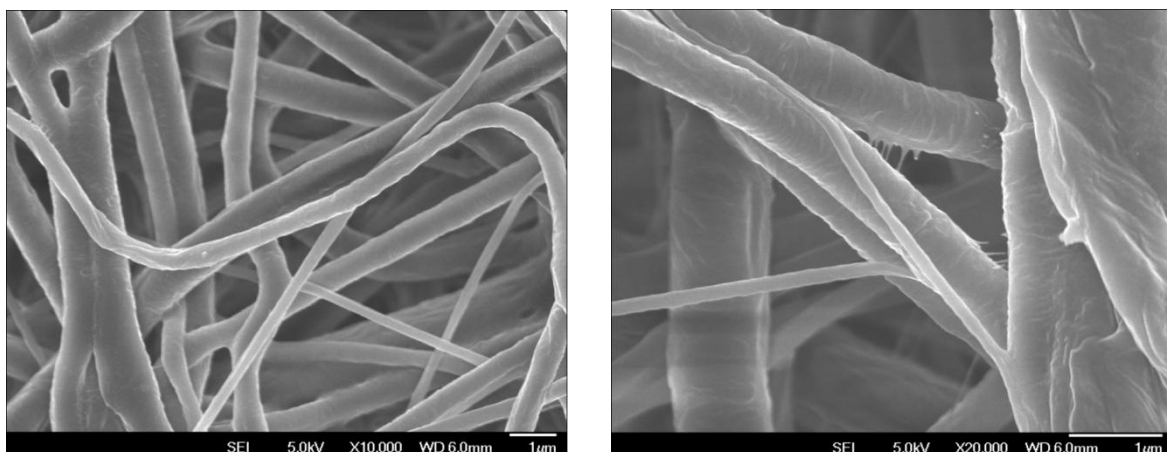


Figure 4.2: FE-SEM images of Polymer A with encapsulation of mixture of Drug 0066, Drug 0350 and Polymer B under 10k magnification (left) and 20k magnification (right).

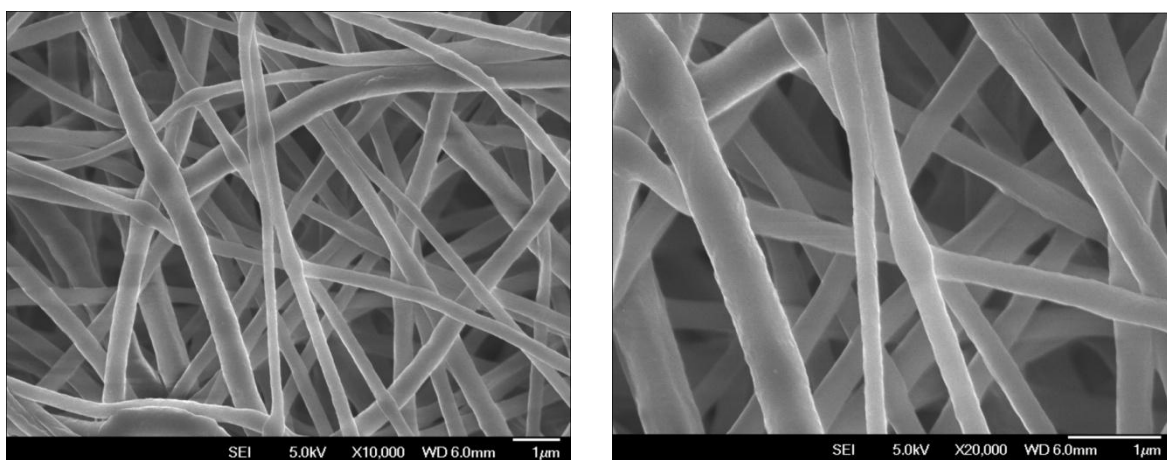


Figure 4.3: FE-SEM images of Polymer A with encapsulation of mixture of Drug 0066 and Drug 0350 under 10k magnification (left) and 20k magnification (right).

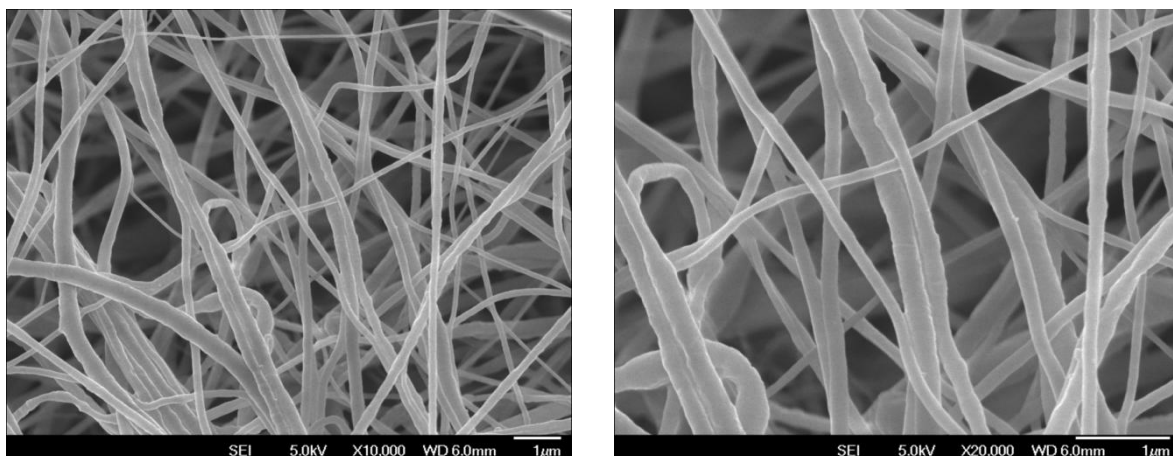


Figure 4.4: FE-SEM images of Polymer A with encapsulation of Drug 0350 under 10k magnification (left) and 20k magnification (right).

Figure 4.2, Figure 4.3 and Figure 4.4 show the nanofibrous morphologies of coaxially electrospun of Polymer A with various encapsulation of mixtures of Drug 0066, Drug 0350 and Polymer B, prepared under stable processing conditions, that are, no dripping of droplet, formation of a stable Taylor cone at the exit orifice of the compound spinneret, and continuous jet ejection during the coaxial electrospinning. All figures were observed under 10k and 20k magnification of FE-SEM. The FE-SEM images illustrate that these nanofibers, despite produced at varied core flow rates and concentration, they possess a common feature of being bead-free, randomly arrayed, and very porous.

As shown in Figure 4.2, Polymer A with encapsulation of mixture of Drug 0066, Drug 0350 and Polymer B was successfully electrospun with the diameter range of 200 nm to 1000 nm. It shows quite uniform fibers without beads with different diameters and amounts of drug entrapment. In the Figure 4.3, the range diameter of electrospun fibers of Polymer A with the encapsulation of mixture of Drug 0066 and Drug 0350 is 200 nm to 600 nm. It shows uniform fibers were formed with bead-free and well alignment structure. From the FE-SEM figures, it can be concluded that Polymer A-Drug 0066/Drug 0350/Polymer B and Polymer A-Drug 0066/Drug 0350 were successfully electrospun under the appropriate and stable conditions. However, for Figure 4.3 of Polymer A with Drug

0350 encapsulation images, even it was electrospun in stable conditions, the fibers formed were not well aligned with a small range diameter of about 100 nm to 400 nm. This is due to the very low viscosity of core solution which leads to electrospaying occurrence. The electrospaying was causing to the production of solution particles instead of nanofibers. Moreover, the presence of distilled water in core solution could affect the formation of electrospun nanofibers because the volatility of solvents is one of the most important influence factors in the solidification of electrospun nanofibers. Since the drug concentration used is 0.4 w/v %, the amount of water content in the core solution is relatively high. The higher the water content, the less uniform the nanofibers in the mats would be. This is because water has relatively low volatility and may not be able to completely evaporate during electrospinning.

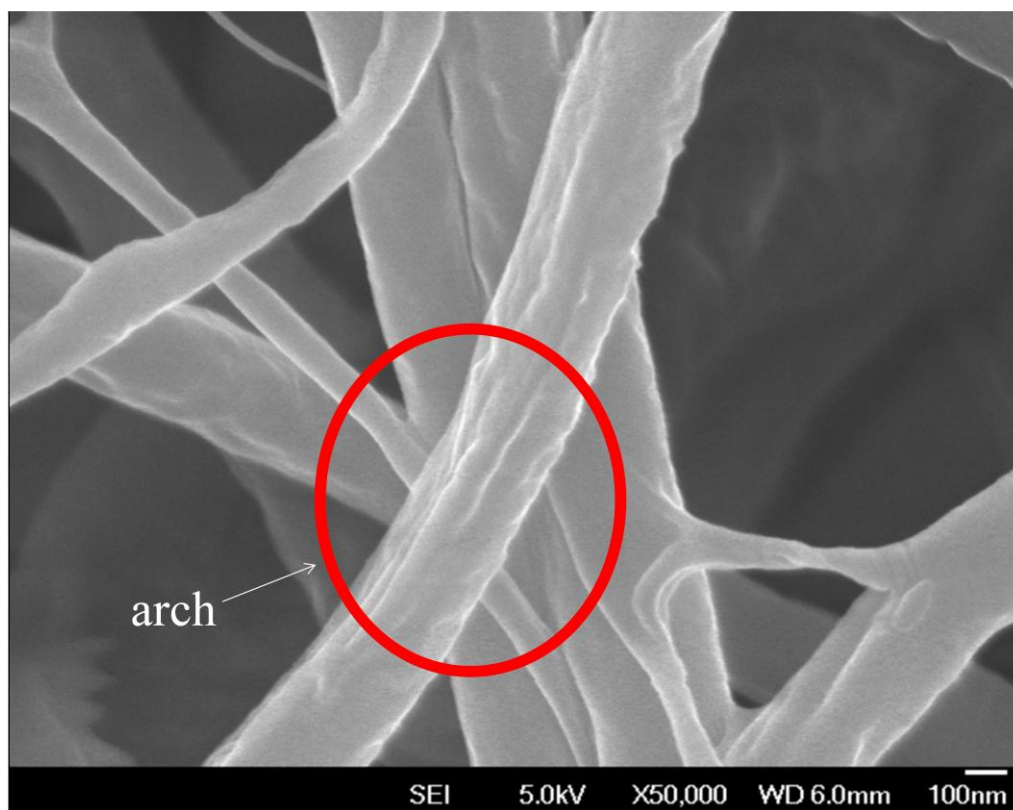


Figure 4.5: FE-SEM images of Polymer A with encapsulation of mixture of Drug 0066, Drug 0350 and Polymer B under 50k of magnification.

Figure 4.5 shows an arch appeared in the FE-SEM images of Polymer A with encapsulation of mixture of Drug 0066, Drug 0350 and Polymer B under 50k of magnification. This arch was proved that the core solution of drugs mixtures was entrapped within the polymer solution. This arch was appeared due to co-axial electrospinning instabilities that lead to imperfections of the electrospun fibers. The core and shell solutions can have a relative velocity, which results from different supply rates determined independently for two syringe pumps. As a result, there might be a distributed longitudinal compression force imposed on the core. Then, the core can buckle. A buckled core can even protrude from the surrounding shell resulting in arch revealed in this experiment.

In the experiment it was found that encapsulation of molecule drugs led to formation of uniform but smaller nanofibrous compared to without encapsulation. The possible reason for this improvement is that addition of drugs disturbed the polymer solution, lowered the surface tension, and thus enhanced the bending instability. Furthermore, measurement of the fiber diameters of all the coaxially electrospun nanofibers indicate that variation of inner flow rate may affect the fiber size. The correlation between flow rate and fiber size increase can be attributed to the extrudate swell effect of viscoelastic polymers in the extrusion process. This is usually affected by factors such as concentration, extrusion rate, nozzle length, addition of stiffer fillers, temperature, etc. The swell effect would be simultaneously passed to the shell fluid by expansion of the shell to a certain extent. This could consequently affect the stretching ability of the jet in the instability development zone. Previous investigations have indicated that the bending instability in the electrospinning is responsible for the formation of nano- or submicroscaled ultrafine fibers. The swell effect would be absent if the inner fluid is not of the viscoelastic type.

4.3 Characterization of the Encapsulation

As the FE-SEM images cannot provide convincing evidences that the drugs were successfully encapsulated inside the nanofibers, several means to characterize this encapsulation effect were employed. First, TEM observation was conducted to obtain direct evidence that various mixtures of drugs were indeed encapsulated within the shell material of Polymer A. As shown in Figure 4.6, the core-shell structured nanofibers composed of Polymer A as shell and the mixture of Drug 0066 and Drug 0350 as core was clearly observed under TEM. Sharp boundaries in the TEM images essentially reflect the difference of electron transmission ability between the core and shell materials. The likely reasons to form sharp boundaries are associated with the immiscibility of the two polymer fluids and the very fast processing characteristic of electrospinning, which would prevent the two fluids from mixing significantly.

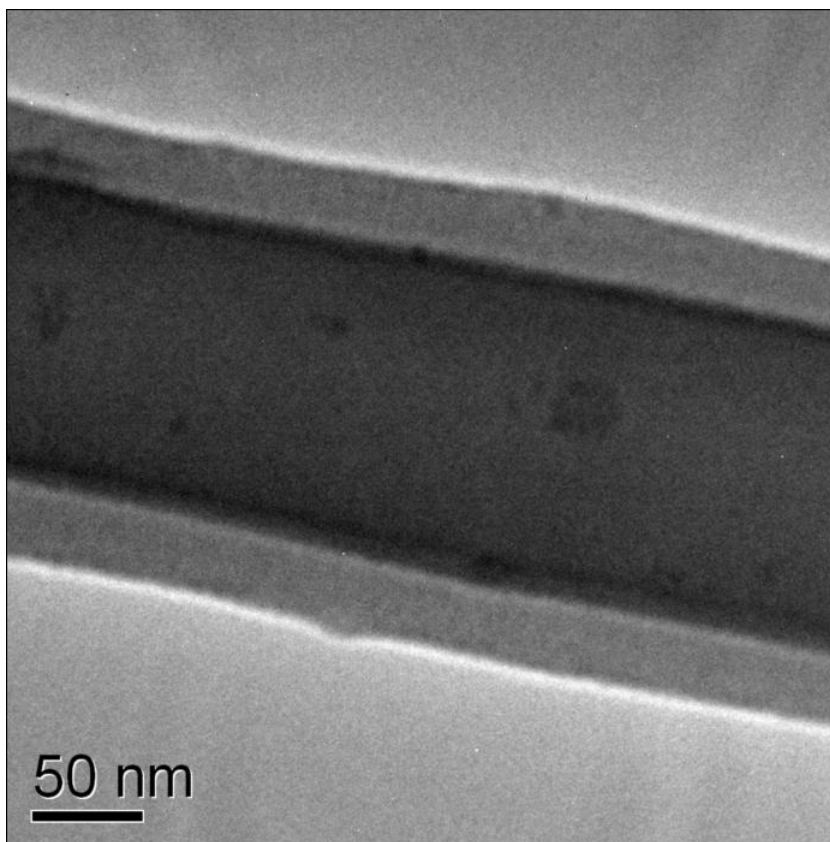


Figure 4.6: Image of core-shell structured nanofibers composed of Polymer A as shell and the mixture of Drug 0066 and Drug 0350 as core under TEM.

Apart from that clearly observed core-shell fibers, TEM images of co-axially electrospun of other various mixture of drugs within Polymer A showed some fibers that did not exhibit any core in the fiber (or the core cannot be seen). Two possible reasons for this phenomenon as suggested by Zhang *et al.* are (1) during the coaxial processing, as happened in a normal electrospinning, there appeared subjects (branching) that were offshoots from the shell fluid of the main compounded fluidic jet. This is true especially for the smaller noncore nanofibers (e.g., diameters <100 nm). (2) It would have a connection with the underlying mechanism of wrapping a core component inside the sheath during the coaxial electrospinning process.

Furthermore, it is suspected that all free charges in the two fluids upon charging would leave the liquid-liquid interface very rapidly and migrate to the outer free surface upon having high potential applied. The Maxwell stress would therefore stretch the outer fluid as that occurring in a normal electrospinning. The inner fluid would be entrained only by the viscous dragging-like stresses and/or contact friction in the inter-phase imposed from the rapid stretching of the shell fluid during coaxial electrospinning. Since the coaxial electrospinning is a dynamic process, factors such as flow rate of the inner and outer fluids, interfacial tension, and viscoelasticity of the two polymer fluids could affect the entrainment and produce noncore fibers. It is suggested that an optimal processing condition may exist where continuous core-shell-structured bicomponent composite nanofibers from the main jet can be produced.

To further confirm the encapsulation of various mixtures of drugs inside Polymer A nanofibers, Fourier Transform InfraRed (FT-IR) test was employed. FT-IR was used in this study is to determine the quality or consistency of the samples. FT-IR has the ability to identify (qualitative analysis) of every different kind of material using infrared spectrum. So to confirm that the electrospun nanofibers were developed through core-shell electrospinning configuration, those co-axial electrospun nanofibers should show the same spectra as electrospun nanofiber of pure Polymer A through FT-IR. This is due to the encapsulation of the core solutions structure by Polymer A, thus the spectra of the polymer will be shown instead of the core solutions' spectra.

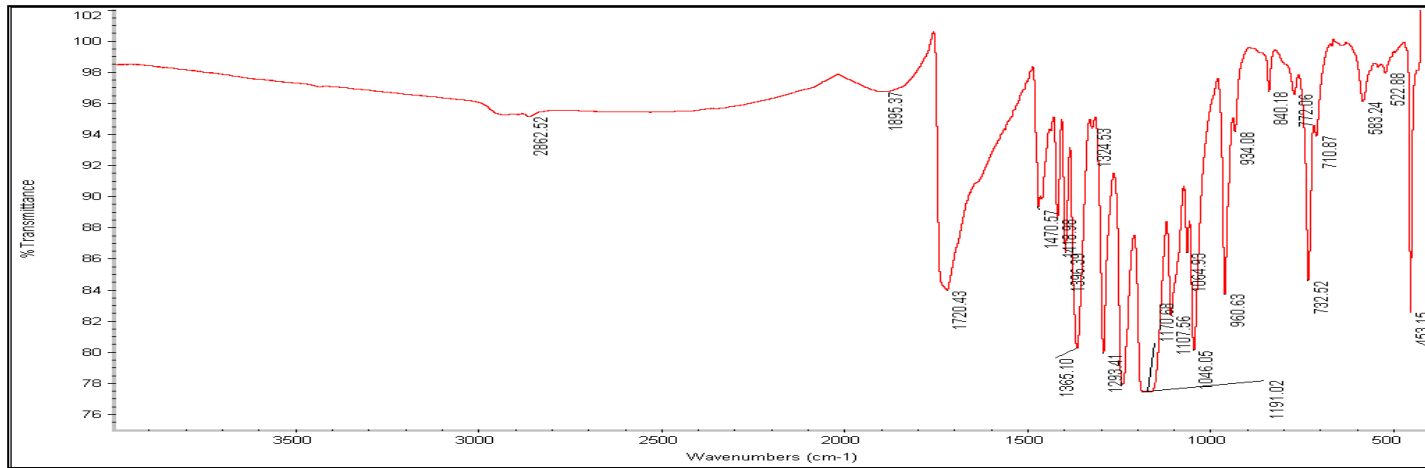


Figure 4.7: FT-IR spectra of electrospun of pure Polymer A.

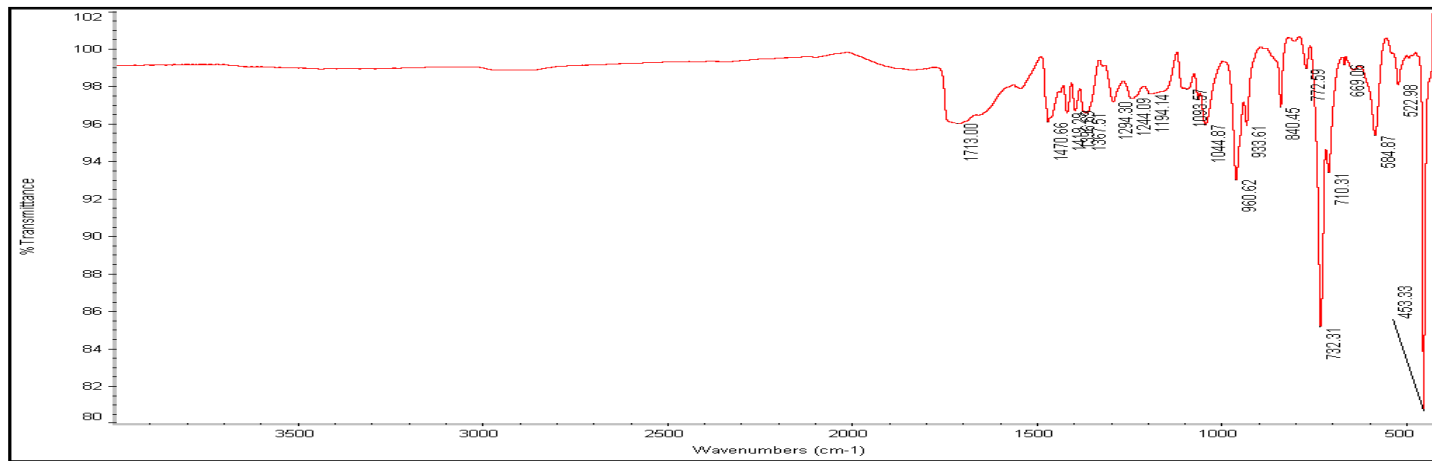


Figure 4.8: FT-IR spectra of electrospun of Polymer A with the encapsulation of mixture of Drug 0066, Drug 0350 and Polymer B.

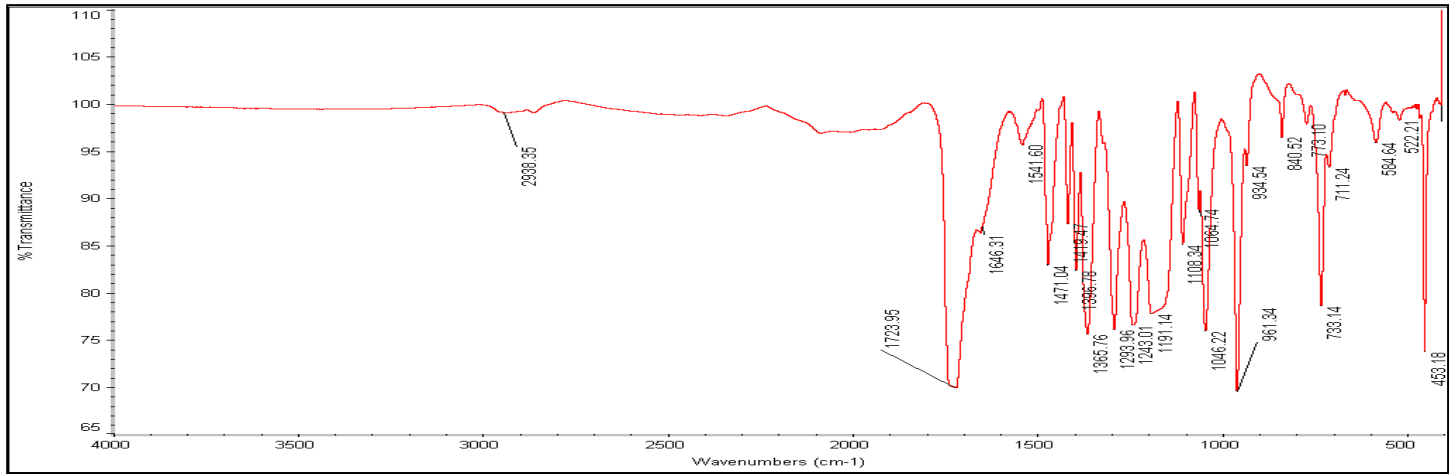


Figure 4.9: FT-IR spectra of electrospun of Polymer A with the encapsulation of mixture of Drug 0066 and Drug 0350.

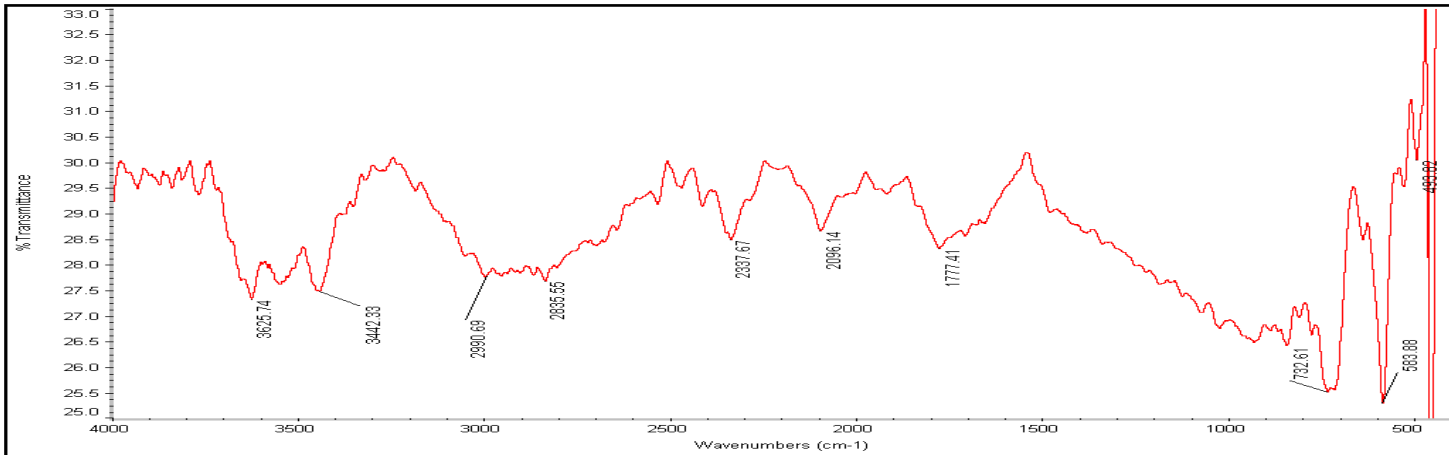


Figure 4.10: FT-IR spectra of electrospun of Polymer A with the encapsulation of Drug 0350.

Figure 4.7 shows FT-IR spectra of electrospun of pure Polymer A used as standard to prove the encapsulation. Each peak represents the bonding of molecules inside the scaffold. To prove the encapsulation, all the molecules' bondings from other scaffolds must have the same bondings as shown in Figure 4.7. For FT-IR spectra of electrospun of Polymer A with the encapsulation of mixture of Drug 0066, Drug 0350 and Polymer B (Figure 4.8), it shows a quite same molecules' bonding but distinct different in peak's height. This is may due to the some of core solutions were mixed with the shell components thus change the height of each peak. A positive result is represented by FT-IR spectra of electrospun of Polymer A with the encapsulation of mixture of Drug 0066 and Drug 0350 (Figure 4.9). The molecules' bonding and the peak's height of the encapsulation scaffold was quite the same. In contrast, FT-IR spectra of electrospun of Polymer A with the encapsulation of Drug 0350 (Figure 4.10) shows a very distinct different between the spectra of electrospun of pure Polymer A. This is because, the core solution of Drug 0350 was mixed with the shell component of Polymer A due the very low viscosity of the drug. Thus, the new molecules' bonding was formed between those solutions and yield a different transmittance from the pure Polymer A spectra.

4.4 Surface Contact Angle

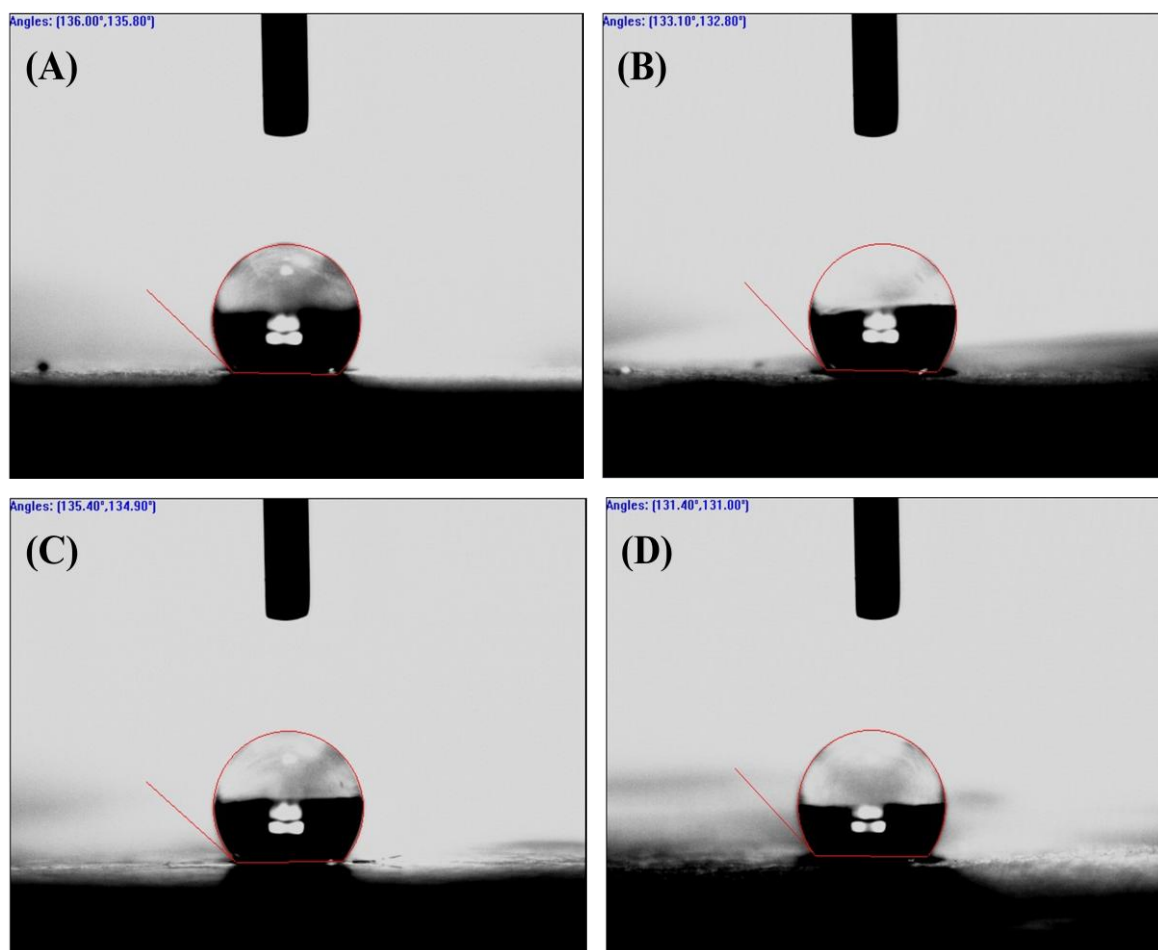


Figure 4.11: Water contact angles on (A) pure Polymer A scaffold, (B) Polymer A with Drug 0066, Drug 0350 and Polymer B encapsulation scaffold, (C) Polymer A with Drug 0066 and Drug 0350 encapsulation scaffold and (D) Polymer A with Drug 0350 encapsulation scaffold.

The hydrophobic (or hydrophilic) nature of a substrate has a direct impact on the avenue of its usage. For tissue-engineering scaffolds hydrophilic scaffolds are preferred. The most direct method of measuring these characteristics is via contact angle measurements.

Surface contact angle of electrospun nanofibrous membranes is simply examined by a water contact angle (WCA) machine. A distilled water pendent droplet is injected from a syringe onto the membrane surface. The image of the droplet on the membrane is visualized through the image analyzer and the angle between the water droplet and the surface is measured. Hydrophilic materials show low contact angle (spreading of water across surface) while hydrophobic materials show high contact angle (minimal contact between droplet and surface).

From Figure 4.11(A), the contact angle of pure Polymer A electrospun fibers is large ($136^\circ \pm 0.5$), indicating the hydrophobicity of such the scaffold. From Figure 4.11(B), 4.11(C) and 4.11(D), the contact angles of each scaffold to water are $133.1^\circ \pm 0.5$, $135.4^\circ \pm 0.5$, and $131.4^\circ \pm 0.5$ respectively. All the encapsulation scaffolds showed the hydrophobic characteristic. All these contact angles measurement showed a desired value as theory since the hydrophilic of the drugs has been encapsulated within the hydrophobic of Polymer A. Thus, all the scaffolds must show the hydrophobic characteristic as shown by Polymer A. The values also showed that all the scaffolds have less contact angle compared to Polymer A's contact angle. This is due the hydrophilicity of drugs component that may be mixed with the Polymer A during the electrospinning process. However, this measurement cannot prove the exact evidence of encapsulation compared to TEM images. This measurement was implemented to determine the hydrophobicity of the samples. Overall, all the samples show the hydrophobic characteristic towards water. Ironically, the tissue engineering prefers hydrophilic scaffolds instead of hydrophobic one. So it is suggested that surface modification techniques have to be employed for the application of this scaffolds.

4.5 *In Vitro* Proteins Release Study

In order to investigate the protein release profile, all the electrospun nanofiber mats samples were first measured using analytical measurement. The samples were then cut about 35-37mg were transferred into the vials containing phosphate buffer saline (PBS) solution (0.05 M, pH 7.4). All vials contained samples were incubated with slowly stirred at

37°C inside the incubator. At predetermined time interval, 1ml of the release medium was collected and analyzed.

The release kinetics of coaxial electrospinning can be illustrated by two stages: an initial fast release before the inflections (stage I) followed by a constant release (stage II). However because of the time constrains, the next phase of the release study was unable to be executed. Based on previous study, reservoir devices have the advantages of providing a constant rate of release over a substantial portion of their lifetime and higher loading level of active agents than most other system. However, reservoir release rate is also critically dependant on shell/coating thickness, surface area, permeability, and defects such as thin spots and pinholes. It was predicted that, Polymer A-Drug 0350 will be the fastest protein release kinetic, followed by Polymer A-Drug 0066/Drug 0350 and Polymer A-Drug 0066/Drug 0350/Polymer B respectively. Polymer A-Drug 0066/Drug 0350/Polymer B will be the slowest protein release kinetic due to the composition of Polymer B that holds and support the proteins inside the core. So, it will take a longer time rather than other scaffolds release.

CHAPTER 5

CONCLUSION AND RECOMMENDATION

5.1 Conclusion

In the conclusion, encapsulation of various mixture of Drug 0066, Drug 0350 and Polymer B within Polymer A electrospun nanofiber for controlled release was successfully developed using co-axial electrospinning. Upon designing the drug delivery systems, a set of experimental designs and parameters such like polymer and shell concentration, solution flow rate, voltage supply and also distance between nozzle's tip to collector were taken into consideration. Co-axial electrospinning setup was used to formulate the drug through reservoir type structure. The morphology of the electrospun nanofibers were observed under FE-SEM and well aligned structure of Polymer A-Drug 0066/Drug 0350/Polymer B and Polymer A-Drug 0066/Drug 0350 were shown. The core-shell structured nanofibers composed of Polymer A-Drug 0066/Drug 0350 was clearly observed under TEM. Besides that, all the electrospun nanofibers with encapsulation showed the hydrophobic characteristic which is similar to the pure electrospun of Polymer A. FT-IR results showed that Polymer A-Drug 0066/Drug 0350/Polymer B and Polymer A-Drug 0066/Drug 0350 have a quite similar peaks compared to the pure electrospun of Polymer A. These similarity properties show that the core components were been encapsulated within the Polymer A. The result indicates that the objectives of this study are achieved.

5.2 Recommendation

It is recommended that large scale production of this drug delivery system to be developed instead of lab scale production by considering GMP guidelines and FDA regulations. The use of core-shell structure nanofibers for encapsulating bioactive substances and conducting controlled releases has yet to be explored.

For the tissue-engineering application, it is recommended that the electrospun nanofibers are treated by plasma treatment for the surface membrane modification. Tissue engineering prefers hydrophilic scaffolds instead of hydrophobic scaffolds to enhance the growth and proliferation of the cells.

Besides that, for commercialize purpose, the toxicity analysis of the polymeric drug delivery systems should be conducted to investigate the safety and health effects of the electrospun nanofibers upon consumption. Apart from that, the drug configuration analysis in terms of bioavailability and bioactivity of the incorporated bioagents should be performed by manipulating the storage period to determine the appropriate shelf life of the electrospun nanofibers for biomedical application especially in therapeutic proteins delivery as proteins denaturation is one of the main concern for such application.

REFERENCES

- Benito, S.M. 2006. *Functionalized polymer nanocontainers for targeted drug delivery*. Ph.D. Thesis. Universität Basel, Argentina.
- Brannon, P.L. 1995. Recent advances on the use of biodegradable microparticles and nanoparticles in controlled drug delivery. *International Journal of Pharmaceutics*.116: 1-9.
- Cambell, D., Pethrick, R. A. and White, J. R. 2000. Chapter 10: scanning electron microscopy polymer characterization, physical techniques (*2nd edition*). Stanley Thornes (Publishers) Ltd. 293-325.
- Casper, C. L., Stephens, J. S., Tassi, N. G., Chase, D. B. and Rabolt, J. F. 2004. Controlling surface morphology of electrospun polystyrene fibers: effect of humidity and molecular weight in the electrospinning process. *Macromolecules*. 37: 573-78.
- Chakraborty, S., Liao, I., Adler, A. and Leong, K. W. 2009. Electrohydrodynamics: a facile technique to fabricate drug delivery systems. *Advance drug delivery reviews*. 61: 1043-54.
- Chen, F., Huang, P. and Mo, X.M. 2010. Electrospinning of heparin encapsulated P(LLA-CL) core/shell nanofibers. *Nano Biomed Eng*. 2: 55-59.
- Deitzel, J.M., Kleinmeyer, J., Harris, D. and Tan, N.C.B. 2001. The effect of processing variables on the morphology of electrospun nanofibers and textiles. *Polymer*. 42(1): 261-72.
- Dietzel, J.M., Kleinmeyer, J.D., Hirvonen, J.K., and Tan, Beck, N.C. 2001. Controlled deposition of electrospun poly (ethylene oxide) fibers. Elsevier Science Ltd.
- Doshi, J. and Renekar D.H. 1995. Electrospinning process and application of electrospun fibers. *J Electrostatics*, 35(2-3): 151-60.
- Guorui, Y. and Wei, Yan. 2011. *The preparation of core/shell nanofibers by electrospinning: applications in tissue engineering and drug delivery*. Ph.D. Thesis. Programs Foundation of Ministry of Education of China.
- Han, D. and Steckl, A. 2009. Superhydrophobic and oleophobic fibers by coaxial electrospinning. *Langmuir*. 25(16): 9454–9462
- Huang, Z., Zhang, Y., Kotaki, M. and Ramakrishna, S. 2003. A review on polymer nanofibers by electrospinning and their applications in nanocomposites. *Composite science and technology*. 63: 2223-53.

- Jaegar, R., Bergshoef, M.M., Battle, C.M.I., Schonherr, H. and Vasco, G.J. 1998. Electrospinning of ultra-thin polymer fibers. *Macromol Symp.* 127: 141-50.
- Jiang, H., Hu, Y., Li, Y., Zhao, P., Zhu, K. and Chen, W. 2005. A facile technique to prepare biodegradable coaxial electrospun nanofibers for controlled release of bioactive agents. *Journal of controlled release.* 108: 237-43.
- Kim, K.K. and Pack, D.W. 2006. *Microspheres for drug delivery.* Springer. 1: 19-50.
- Lee, Y.S. and Arinze, T.L. 2011. Review: Electrospun Nanofibrous Materials for Neural Tissue Engineering. *Polymers.* 3: 413-26.
- Martin, P. 2006. Beyond the next generation of therapeutic protein (online). <http://www.biotech-online.com/fileadmin/artimg/beyond-the-next-generation-of-therapeutic-proteins.pdf> (15 Nov 2011)
- Megelski, S., Stephens, J.S., Chase, D.B., and Rabolt, J.F. 2002. Micro and Nanostructured surface morphology on electrospun polymer fibers. *Macromolecules.* 35(22): 8456-66.
- Mo, X., Xu, C., Kotaki, M. and Ramakrishna, S. 2004. Electrospun P(LLA-CL) nanofiber: A biomimetic extracellular matrix for smooth muscle cell and endothelial cell proliferation. *Biomaterials.* 25: 1883-90.
- Li, D. and Xia, Y. 2004. Electrospinning of nanofibers: reinventing the wheel. *Adv Mater.* 16(14): 1151-70.
- Lu, P. and Ding, B. 2008. Applications of electrospun fibers. *Recent Patents on Nanotechnology.* 2: 169-82.
- Pham, Q.P., Upma, S. and Antonios, G.M. 2006. Electrospinning of Polymeric Nanofiber for Tissue Engineering Applications: A Review.
- Ramakrishna, S., Fujihara, K. Teo, W., Lim, T. and Ma, Z. 2005. *An introduction to electrospinning and nanofibers,* World Scientific Publishing Co. Pte. Ltd.
- Rao, S.S. 2004. *Electrospun PLLA/SWNT Nanocomposite Fibril for Cartilage Regeneration.* Master. Thesis. Drexel University, Pennsylvania, USA.
- Rao, V.S. 2009. *Collection of highly aligned electrostrictive graft elastomer nanofibers using electrospinning in a vacuum environment.* Master. Thesis. Kansas State University Manhattan, Kansas.
- Sahoo, S., Ang, L.T., Goh, J.C.H. and Toh, S.L. 2009. Growth factor delivery through electrospun nanofibers in scaffolds for tissue engineering applications. *Journal of Biomedical Materials Research.* 1539-50

- Sill, T. and von Recum, H. (2008). Electrospinning: Applications in drug delivery and tissue engineering, *Biomaterials*. 29: 1989-2006.
- Subbiah, T., Bhat, G.S., Tock, R.W., Parameswaran, S. and Ramkumar, S.S. 2004. Electrospinning of Nanofibers. *Journal of Applied Polymer Science*. 96: 557-59.
- Warner, S.B., Buer, A., Grimler, M., Ugbohue, S.C., Rutledge, G.C. and Shin, M.Y. 1999. A fundamental investigation of the formation and properties of electrospun fibers (online). <http://heavenly.mit.edu/rutledge/PDFs/NTCannual99.pdf>. (20 August 2011)
- Wang, H.S., Fu, G.D. and Li, X.S. 2009. Functional Polymeric Nanofibers from Electrospinning. *Recent Patents on Nanotechnology*. 3: 21-31.
- Xu, X., Chen, X., Ma, P., Wang, X. and Jing, X. 2008. The release behaviour of doxorubicin hydrochloride from medicated fibers prepared by emulsion-electrospinning. *European journal of pharmaceutics and biopharmaceutics*. 70: 165-70.
- Xu, X., Yang, L., Xu, X., Wang, X., Chen, X., Liang, Q., Zeng, J. and Jing, X. 2005. Ultrafine medicated fibers electrospun from W/O emulsions. *Journal of controlled release*. 108: 33-42.
- Yarin, A.L. 2010. Review: Coaxial electrospinning and emulsion electrospinning of core-shell fibers. *Polymer Advance Technology*. 22: 310-17.
- Yih, T.C. and Al-Fandi, M. 2006. Engineered nanoparticles as precise drug delivery system. *Journal of Cellular Biochemistry*. 97:1184-90.
- Yuan, X., Zhang, Y., Dong, C. and Sheng, J. 2005. Morphology of ultrafine polysulfone fibers prepared by electrospinning. *Polymer, In Press*.

- Zhao, S., Wu, X., Wang, L. and Huang, Y. 2004. Electrospinning of ethyl-cyanoethyl cellulose/tetrahydrofuran solutions, *Journal of applied polymer science*. 91: 242-46.
- Zhang, Y. Z., Wang, X., Feng, Y., Li, J., Lim, C.T. and Ramakrishna, S. 2006. Coaxial Electrospinning of (Fluorescein Isothiocyanate-Conjugated Bovine Serum Albumin)-Encapsulated Poly(E-caprolactone) Nanofibers for Sustained Release. *Biomacromolecules*. 7: 1049-1057.

APPENDICES

Electrospinning Process:

All coaxial electrospinning processes have been done using coaxial electrospinning setup using 25G needle for inner and 16G needle for outer capillary.

1) Polymer A-Drug 0066/Drug 0350/Polymer B

SET 1

Shell solution: 1.212g of Polymer A + 10ml of TFE

Core solution: 0.014g of Drug 0066 dissolved in 10.3 of 10wt% of Polymer B + 100 μ l of 40mg of Drug 0350 in 10ml of water/dimethyl formamide solution.

Parameters applied:

Voltage supply (kV)	Distance between tip's and collector (cm)	Core solution flow rate (ml/h)	Shell solution flow rate (ml/h)
10.6	13	0.45	1.8

SET 2

The same shell and core solution were used as above.

Parameters applied:

Voltage supply (kV)	Distance between tip's and collector (cm)	Core solution flow rate (ml/h)	Shell solution flow rate (ml/h)
11.9	13	0.60	1.8
11.9	13	0.30	1.8
11.9	13	0.30	1.0
13.5	13	0.30	1.0
16.5	13	0.50	1.5
17.1	13	0.50	1.5

SET 3

Shell solution: 2.103g of Polymer A + 9.1ml of chloroform + 4.7 of methanol

Core solution: 0.014g of Drug 0066 dissolved in 10.3 of 10wt% of Polymer B + 100 μ l
40mg of Drug 0350 in 10ml of water/dimethyl formamide solution.

Parameters applied:

Voltage supply (kV)	Distance between tip's and collector (cm)	Core solution flow rate (ml/h)	Shell solution flow rate (ml/h)
17.1	13	0.30	1.6

SET 4

Shell solution: 1.212g of PCL + 10ml of TFE

Core solution: 0.500g of BSA dissolved in 10mg of 5wt% of PVA + 1ml of 30.2mg of curcumin in 10ml of ethanol solution.

Voltage supply (kV)	Distance between tip's and collector (cm)	Core solution flow rate (ml/h)	Shell solution flow rate (ml/h)
16.0	13	0.60	1.8
16.0	13	0.30	1.8
16.0	13	0.10	1.8
19.0	13	0.10	1.8
19.0	13	0.10	1.5

2) Polymer A-Drug 0066/Polymer B

SET 1

Shell solution: 1.212g of Polymer A + 10ml of TFE

Core solution: 0.014g of Drug 0066 dissolved in 10.3 of 10wt% of Polymer B

Parameters applied:

Voltage supply (kV)	Distance between tip's and collector (cm)	Core solution flow rate (ml/h)	Shell solution flow rate (ml/h)
10.6	13	0.60	1.8
10.6	13	0.45	1.8

3) Polymer A-Drug 0066/Drug 0350

SET 1

Shell solution: 1.8201g of Polymer A + 15ml of TFE

Core solution: 0.500g of Drug 0066 dissolved in 10ml of DI water + 1ml of 30.2mg of Drug 0350 in 10ml of ethanol solution.

Parameters applied:

Voltage supply (kV)	Distance between tip's and collector (cm)	Core solution flow rate (ml/h)	Shell solution flow rate (ml/h)
12.5	13	0.60	1.8
12.5	13	0.30	1.8
12.5	13	0.15	1.8
13.3	13	0.15	1.8
15.5	13	0.15	1.8

4) Polymer A-Drug 0350

SET 1

Shell solution: 1.212g of Polymer A + 10ml of TFE

Core solution: 40mg of Drug 0350 in 10ml of water/dimethyl formamide

Parameters applied:

Voltage supply (kV)	Distance between tip's and collector (cm)	Core solution flow rate (ml/h)	Shell solution flow rate (ml/h)
10.6	13	0.40	1.4

SET 2

Shell solution: 1.212g of Polymer A + 10ml of TFE

Core solution: 30.2mg of Drug 0350 in 10ml of ethanol.

Parameters applied:

Voltage supply (kV)	Distance between tip's and collector (cm)	Core solution flow rate (ml/h)	Shell solution flow rate (ml/h)
12.3	13	0.15	1.8
13.3	13	0.15	1.8
11.1	13	0.15	1.8
15.5	13	0.15	1.8
14.2	13	0.15	1.8
13.1	15	0.15	1.4
13.1	12.5	0.15	1.4
11.1	12.5	0.15	1.4
10.0	12.5	0.15	1.4
11.3	12.5	0.09	1.4
13.5	12.5	0.09	1.4
9.3	12.5	0.09	1.4
9.3	13.5	0.09	1.4
9.2	13.5	0.15	1.8
10.7	13.5	0.15	1.8
16.1	13.5	0.15	1.8
13.9	13.5	0.15	1.8
12.9	13.5	0.15	1.8
12.9	13.5	0.30	1.8
12.9	13.5	0.45	1.8
13.1	13.5	0.35	1.8
12.9	13	0.20	1.5
12.9	13	0.13	1.3

14.5	13	0.20	1.5
15.0	13	0.20	1.5
14.0	13	0.20	1.5
14.9	13	0.20	1.5
13.6	13	0.20	1.5

5) Polymer A (control) using simple electrospinning setup

SET 1

Solution: 2.103g of PCL + 9.1ml of chloroform + 4.7 of methanol

Parameters applied:

Voltage supply (kV)	Distance between tip's and collector (cm)	Solution flow rate (ml/h)
19	14	1.2

SET 2

Solution: 1.212g of Polymer A + 10ml of TFE

Parameters applied:

Voltage supply (kV)	Distance between tip's and collector (cm)	Solution flow rate (ml/h)
19	14	1.2
15	14	1.2